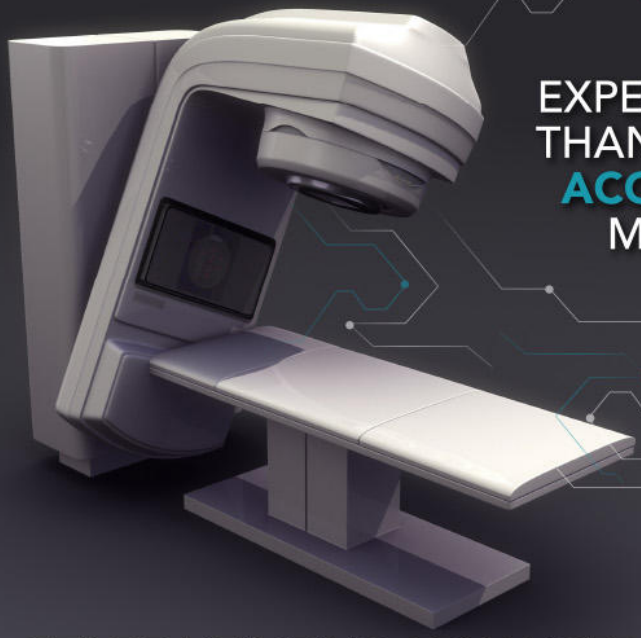

EXPECT NOTHING LESS THAN **SUB-MILLIMETER ACCURACY** IN YOUR MEASUREMENTS

RIT®

START UTILIZING ADVANCED PRECISION QA TODAY

THE RIT FAMILY OF PRODUCTS **VERSION 6.7.X**

3D Winston-Lutz Isocenter Optimization
The enhanced isocenter optimization routine allows for optimal cone detection, resulting in the utmost precision. The accuracy of this routine now surpasses sub-millimeter resolution. *(Pictured above)*

Cerberus 2.0: The Future of Complete Automation
Completely streamline your automated phantom analysis workflow with the new Cerberus. Cerberus operates in the background of your workstation, allowing for hands-free Imaging QA.

One-Click, Instant Automated Phantom Analyses

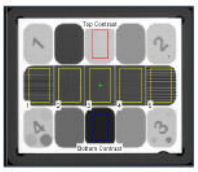

RIT's full suite of phantom analyses provides fast, robust, and accurate analysis of all imaging tests recommended in TG-142. The software now offers added support for the QCkV-1 phantom. *(Pictured right)*

Tolerance Customization and Management
RIT's new Tolerance Manager offers comprehensive customization of tolerance values for every measurement used in all automated phantom analyses. Tolerance profiles can be precisely-tailored to each individual machine in use.

CLICK HERE TO DOWNLOAD TODAY

Elekta Leaf Speed Analysis
RIT now offers fast and accurate automated analysis for Elekta MLC QA. The new Leaf Speed Analysis routine measures the consistency and accuracy of the MLC leaf speeds as they traverse the imager.

TomoTherapy® Registration for Patient QA
Easily perform exact dose comparisons with RIT's new TomoTherapy Registration routine. This new, innovative wizard uses a TomoTherapy® plan, dose map, and a film to determine position an dose accuracy using the red lasers. *(Pictured below)*

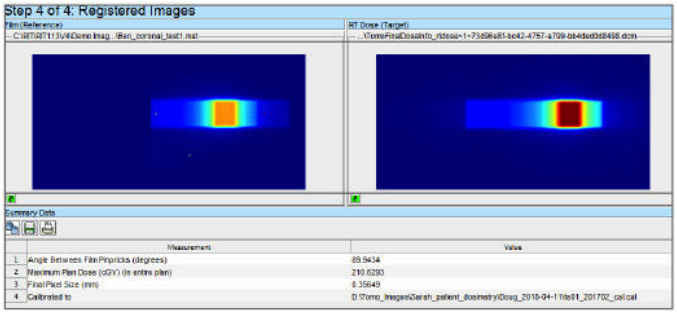

Streamline Your QA Workflow
Fully-customize your software experience with RIT's updated and dynamic interface. With the new ability to hide/display any features or sections, you can instantly access you most frequently-performed analysis routines.

Convenient, Cloud-Based Software Licensing
Easily manage your software licenses with RIT's new, flexible system at your convenience, 24/7/365 without the help of RIT Technical Support. Upgrading is now easier than ever.

RADIOLOGICAL IMAGING TECHNOLOGY, INC.
RADIMAGE.COM
(+1) 719.590.1077 x211 // sales@radimage.com

Connect with RIT
@RIT4QA

Supplement to the 2004 update of the AAPM Task Group No. 43 Report

Mark J. Rivard[a)]
Department of Radiation Oncology, Tufts University School of Medicine, Boston, Massachusetts 02111

Wayne M. Butler
Schiffler Cancer Center, Wheeling Hospital, Wheeling, West Virginia 26003

Larry A. DeWerd
Accredited Dosimetry and Calibration Laboratory, University of Wisconsin, Madison, Wisconsin 53706

M. Saiful Huq
Department of Radiation Oncology, University of Pittsburgh Cancer Institute, Pittsburgh, Pennsylvania 15232

Geoffrey S. Ibbott
Radiological Physics Center, M.D. Anderson Cancer Center, Houston, Texas 77030

Ali S. Meigooni
Department of Radiation Medicine, University of Kentucky Medical Center, Lexington, Kentucky 40536

Christopher S. Melhus
Department of Radiation Oncology, Tufts University School of Medicine, Boston, Massachusetts 02111

Michael G. Mitch
Ionizing Radiation Division, National Institute of Standards and Technology, Gaithersburg, Maryland 20899

Ravinder Nath
Department of Therapeutic Radiology, Yale University School of Medicine, New Haven, Connecticut 06510

Jeffrey F. Williamson
Department of Radiation Oncology, Virginia Commonwealth University, Richmond, Virginia 23298

(Received 3 January 2007; revised 19 March 2007; accepted for publication 9 April 2007; published 24 May 2007)

Since publication of the 2004 update to the American Association of Physicists in Medicine (AAPM) Task Group No. 43 Report (TG-43U1), several new low-energy photon-emitting brachytherapy sources have become available. Many of these sources have satisfied the AAPM prerequisites for routine clinical use as of January 10, 2005, and are posted on the Joint AAPM/RPC Brachytherapy Seed Registry. Consequently, the AAPM has prepared this supplement to the 2004 AAPM TG-43 update. This paper presents the AAPM-approved consensus datasets for these sources, and includes the following ^{125}I sources: Amersham model 6733, Draximage model LS-1, Implant Sciences model 3500, IBt model 1251L, IsoAid model IAI-125A, Mentor model SL-125/SH-125, and SourceTech Medical model STM1251. The Best Medical model 2335 ^{103}Pd source is also included. While the methodology used to determine these data sets is identical to that published in the AAPM TG-43U1 report, additional information and discussion are presented here on some questions that arose since the publication of the TG-43U1 report. Specifically, details of interpolation and extrapolation methods are described further, new methodologies are recommended, and example calculations are provided. Despite these changes, additions, and clarifications, the overall methodology, the procedures for developing consensus data sets, and the dose calculation formalism largely remain the same as in the TG-43U1 report. Thus, the AAPM recommends that the consensus data sets and resultant source-specific dose-rate distributions included in this supplement be adopted by all end users for clinical treatment planning of low-energy photon-emitting brachytherapy sources. Adoption of these recommendations may result in changes to patient dose calculations, and these changes should be carefully evaluated and reviewed with the radiation oncologist prior to implementation of the current protocol. [DOI: 10.1118/1.2736790]

Key words: brachytherapy, dosimetry protocol, TG-43

I. INTRODUCTION

The 1995 report from the American Association of Physicists in Medicine (AAPM) Task Group No. 43 (TG-43)[1] on the dosimetry of interstitial brachytherapy sources was updated in 2004, and was termed the AAPM TG-43U1 report.[2–6] The 1995 report contained recommended datasets for four interstitial brachytherapy sources: Amersham-Health models 6702 and 6711 sources of ^{125}I, the Theragenics Corporation

model 200 source of ^{103}Pd and the Best Medical ^{192}Ir source (certain commercial equipment, instruments, and materials are identified in this work in order to specify adequately the experimental procedure. Such identification does not imply recommendation nor endorsement by either the AAPM or National Institute of Standards and Technology (NIST), nor does it imply that the material or equipment identified is necessarily the best available for these purposes). In the 2004 update, the AAPM updated the data on the ^{125}I and ^{103}Pd sources included in the original report and included data on six other interstitial brachytherapy sources. All of the following eight sources met the AAPM dosimetric prerequisites[7] and the AAPM Calibration Laboratory Accreditation (CLA) subcommittee requirements[8] as of July 15, 2001 and were presented in the AAPM TG-43U1 report:

1 Amersham-Health model 6702 ^{125}I source,
2. Amersham-Health model 6711 ^{125}I source,
3. Best Medical model 2301 ^{125}I source,
4. North American Scientific Inc. (NASI) model MED3631-A/M ^{125}I source,
5. Bebig/Theragenics model I25.SO6 ^{125}I source,
6. Imagyn isostar model IS-12501 ^{125}I source (note that the Imagyn isostar model IS-12501 ^{125}I source which was included in the 2004 AAPM TG-43U1 report has been removed from the online Joint AAPM/RPC Source Registry due to discontinuation by the manufacturer),
7. Theragenics Corporation model 200 ^{103}Pd source, and
8. NASI model MED3633 ^{103}Pd source.

Since July 15, 2001 several additional sources have been introduced in the market and have met the AAPM dosimetric prerequisites and the CLA subcommittee requirements. As planned during the writing of TG-43U1, a supplement was needed to present consensus datasets for these newer sources. This supplement is termed TG-43U1S1, and includes the following sources which met the criteria mentioned above as of January 10, 2005:

1. Amersham model 6733 ^{125}I source,
2. DraxImage model LS-1 ^{125}I source,
3. Implant Sciences model 3500 ^{125}I source,
4. IBt model 1251L ^{125}I source,
5. IsoAid model IAI-125A ^{125}I source,
6. Mills Biopharmaceuticals model SL-125/SH-125 ^{125}I source,
7. SourceTech Medical model STM1251 ^{125}I source, and
8. Best Medical model 2335 ^{103}Pd source.

Manufacturers, dosimetry investigators, and end users have generally adhered to AAPM recommendations given in the TG-43U1 and CLA subcommittee reports. The source models reviewed in this supplement (Fig. 1) satisfied AAPM recommendations (dosimetric parameters accepted for publication in a scientific, peer-reviewed journal and metrologically acceptable source calibration procedures) on or before January 10, 2005. After review and approval, these data were posted on the online Joint AAPM/RPC Source Registry.[9] As stated in the AAPM TG-43U1 report, publications may report dosimetry parameters using Monte Carlo, experimental methods, or both techniques in the same publication. It is also worth stressing that special care is needed to address concerns for independence of various investigations included in the development of consensus datasets. The independence policy is described in detail in Sec. V F of the AAPM TG-43U1
report.

II. CONSENSUS DATASETS FOR CLINICAL IMPLEMENTATION

As presented in the TG-43U1 report, criteria used to evaluate dosimetry parameters for each source model included in this TG-43U1S1 report were:

1. Internal source geometry and a description of the source,
2. review of the pertinent literature for the source,
3. correction to Λ values due to the 1999 anomaly in NIST air-kerma strength measurements (if applicable),
4. solid water-to-liquid water corrections,
5. experimental method used: TLD or diode,
6. active length assumed for the geometry function line-source approximation,
7. name and version of the Monte Carlo transport code,
8. cross-section library used by the Monte Carlo simulation,
9. Monte Carlo estimator used to score kerma or dose, and
10. agreement between Monte Carlo calculations and experimental measurement.

AAPM-approved consensus datasets are provided in Tables I–X below with calculated dose rates using the one-dimensional (1D) formalism in Table XI as similar to the 2004 AAPM TG-43U1 report. Descriptions of each source and details used for obtaining the consensus datasets are available in Appendix A. If essential items critical to the evaluation of a given source were omitted from the salient publications, then dosimetry investigators were contacted for additional information and/or clarification. Fortunately, in recent publications, analysis for some of these source models benefited from adherence by dosimetry investigators to recommendations provided in Secs. V D and V E of the AAPM TG-43U1 report. Data were *italicized* if they were not directly confirmed by other measurements or calculations; **boldface** values indicate that data were interpolated towards presenting data sets of all sources on a common mesh; extrapolated data are underlined. As in the 2004 report, data sets were thinned so as to minimize the amount of data while maintaining interpolation errors $\leqslant 2\%$ for the purposes of calculating dose rate distributions. Due to differences in source construction, appropriate angular resolution for $F(r,\theta)$ was used to keep bilinear interpolation errors $\leqslant 2\%$.

Additionally, the AAPM TG-43U1 report recommended a mass density of 0.001 20 g cm^{-3} for both moist and dry air. Upon analyzing the impact of relative humidity from 0% to 100%, a value of 0.001 19 g cm^{-3} is more appropriate and should be used in conjunction with the recommended relative humidity of 40%.

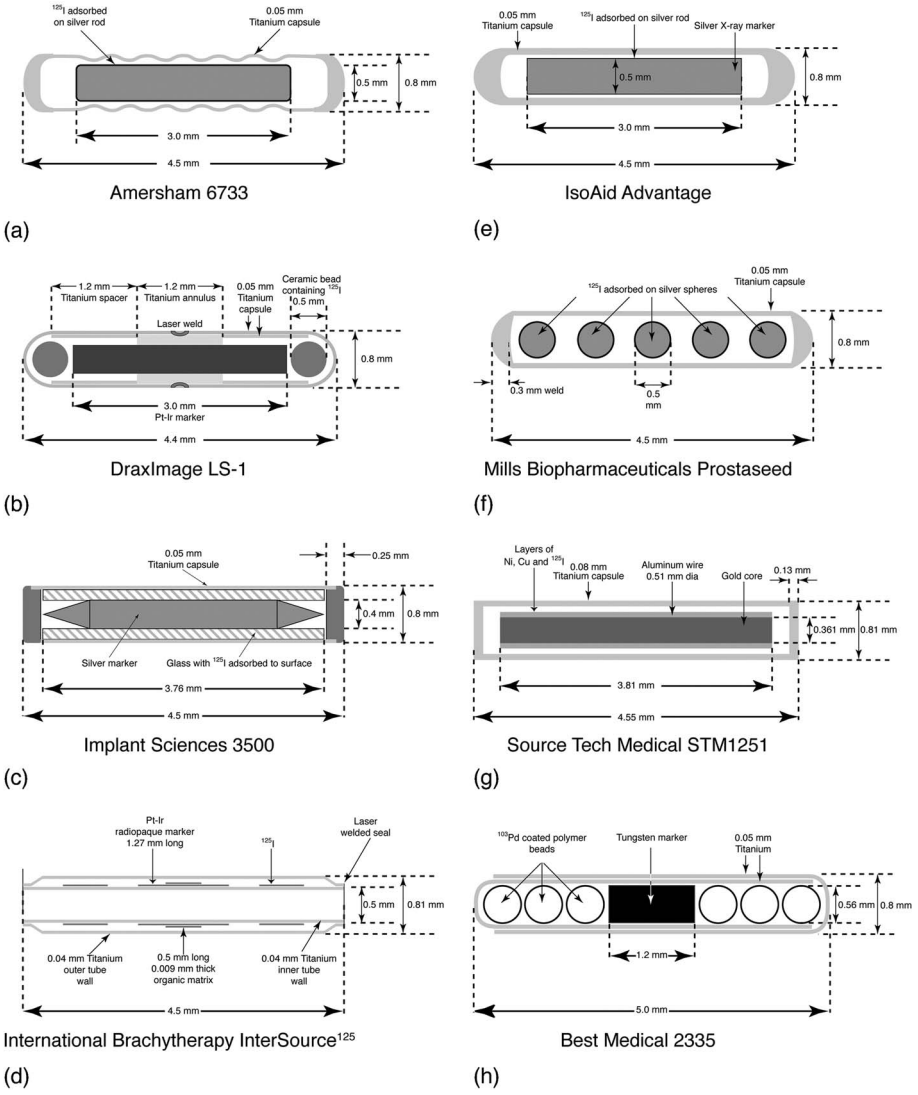

FIG. 1. Brachytherapy seeds examined in this report: (a) Amersham model 6733 source, (b) DraxImage model LS-1 source, (c) Implant Sciences model 3500 source, (d) International Brachytherapy model 1251L source, (e) IsoAid model IAI-125A source, (f) Mills Biopharmaceuticals Corporation model SL-125/SH-125 source, (g) Source Tech Medical model STM 1251 source, and (h) Best Medical model 2335 source. Titanium capsule wall thicknesses are 0.08, 0.07, and 0.04 mm for the SourceTech Medical, Best, and IBt seeds, respectively. Capsule wall thickness for the remaining seeds is 0.05 mm.

III. CLARIFICATIONS ON RECOMMENDED INTERPOLATION AND EXTRAPOLATION METHODS

While a sampling space with uniform increments for $g(r)$ and either $F(r,\theta)$ or $\phi_{an}(r)$ is desired, the published data indicate that authors have used a variety of spatial and angular increments and ranges. Therefore, interpolation or extrapolation may be required to determine dose rate distributions at spatial locations not explicitly included in published dosimetry-parameter tables. Methods for determining dose rates at positions not characterized by the available datasets or related publications were specified in the 2004 AAPM TG-43U1 report. Interpolation methods for 2D and 1D dosimetry parameters were provided in Sec. IV. (g) of the 2004

TABLE I. NIST standard WAFAC calibration dates for air-kerma strength for each manufacturer, and dose rate constant values.

Manufacturer and source type		Date used by NIST and ADCLs for calibration	${}_{\text{CON}}\Lambda$ $[\text{cGy}\cdot h^{-1}\cdot U^{-1}]$
Amersham 6733	^{125}I	February 15, 2001	0.980
Draximage LS-1	^{125}I	January 13, 2001	0.972
Implant Sciences 3500	^{125}I	April 22, 2000	1.014
IBt 1251L	^{125}I	May 17, 2000	1.038
IsoAid IAI-125A	^{125}I	April 15, 2001	0.981
MBI SL-125/SH-125	^{125}I	July 5, 2001	0.953
SourceTech Medical STM1251	^{125}I	June 2, 2000	1.018
Best Medical 2335	^{103}Pd	September 2, 2000	0.685

TABLE II. AAPM Consensus L, $g_L(r)$, and $g_P(r)$ values for seven ^{125}I sources and one ^{103}Pd source (i.e., Best Medical model 2335). As used later in Table XI, $\phi_{an}(r)$ data are given in the lowest five rows. Interpolated data are **boldface**, extrapolated data are underlined, and *italicized* data are obtained from candidate datasets.

	Line source approximation							
L (mm)	3.0	4.1	3.76	4.35	3.0	3.0	3.81	4.55
r(cm)	Amersham EchoSeed 6733	Draximage BrachySeed LS-1	Implant Sciences 3500	IBt 1251L	IsoAid advantage IAI-125A	MBI SL-125 SH-125	Source Tech STM1251	Best Medical 2335
0.10	1.050	0.182	*0.997*	0.757	*1.040*	1.101	0.941	*0.826*
0.15	1.076	**0.323**	*1.011*	**0.841**	***1.053***	1.101	**0.972**	*1.066*
0.25	1.085	*0.741*	*1.021*	**0.963**	**1.066**	**1.101**	**1.013**	*1.236*
0.50	1.069	0.964	*1.030*	1.021	1.080	1.084	1.033	1.307
0.75	1.045	1.004	1.026	**1.024**	***1.035***	**1.041**	1.022	**1.128**
1.00	1.000	1.000	1.000	1.000	1.000	1.000	1.000	1.000
1.50	0.912	0.937	0.932	0.937	0.902	0.898	0.937	0.742
2.00	0.821	0.853	0.854	0.859	0.800	0.795	0.856	0.533
3.00	0.656	0.680	0.681	0.700	0.611	0.610	0.691	0.296
4.00	0.495	0.527	0.532	0.554	0.468	0.456	0.540	0.158
5.00	0.379	0.400	0.407	0.425	0.368	0.338	0.415	0.0920
6.00	0.285	0.300	0.308	0.323	0.294	0.250	0.314	*0.0529*
7.00	0.214	0.223	0.230	0.240	0.227	0.183	0.236	*0.0309*
8.00	0.155	0.166	0.171	0.180	0.165	0.134	0.176	0.0180
9.00	0.119	0.122	0.127	0.138	0.141	0.098	0.131	0.0105
10.00	0.0840	0.0900	0.0936	0.101	*0.090*	0.072	0.0969	0.0062
	Point source approximation							
0.10	0.693	0.100	*0.576*	0.403	*0.686*	0.727	0.544	*0.427*
0.15	0.851	**0.225**	*0.732*	**0.569**	**0.833**	0.871	**0.700**	*0.706*
0.25	0.985	*0.629*	*0.886*	**0.805**	***0.967***	**0.999**	**0.876**	*1.020*
0.50	1.046	0.928	*0.997*	0.978	1.056	1.061	0.999	1.247
0.75	1.039	0.994	1.017	**1.012**	***1.029***	**1.035**	1.013	**1.114**
1.00	1.000	1.000	1.000	1.000	1.000	1.000	1.000	1.000
1.50	0.916	0.944	0.938	0.945	0.906	0.901	0.943	0.749
2.00	0.826	0.862	0.862	0.869	0.804	0.799	0.864	0.539
3.00	0.660	0.688	0.688	0.710	0.615	0.614	0.698	0.300
4.00	0.498	0.534	0.538	0.562	0.471	0.459	0.546	0.161
5.00	0.382	0.405	0.412	0.432	0.371	0.340	0.420	0.0935
6.00	0.287	0.304	0.312	0.328	0.296	0.252	0.318	*0.0538*
7.00	0.216	0.226	0.233	0.244	0.229	0.184	0.239	*0.0314*
8.00	0.156	0.168	0.173	0.183	0.166	0.135	0.178	0.0184
9.00	0.120	0.124	0.129	0.141	0.142	0.099	0.133	0.0107
10.00	0.0846	0.0912	0.0947	0.102	0.091	0.072	0.0980	0.0063
$\phi_{an}(0.10)$	1.173	2.004	1.129	1.162	1.127	1.091	1.172	1.052
$\phi_{an}(0.15)$	1.246	2.275	1.268	1.327	1.197	1.159	1.317	1.205
$\phi_{an}(0.25)$	1.112	2.152	1.164	1.296	1.069	1.035	1.210	1.213
$\phi_{an}(0.50)$	0.996	1.150	0.973	1.028	0.957	0.927	0.982	0.938
$\phi_{an}(0.75)$	0.974	1.030	**0.942**	**0.992**	**0.962**	0.907	**0.962**	0.894

AAPM TG-43U1 report, and extrapolation methods for these same parameters were provided in its Appendix C. Linear-linear interpolation was recommended for $F(r,\theta)$, and log-linear interpolation was recommended for $g(r)$. However, specific guidance on implementation of these recommendations by medical physicists or treatment planning software manufacturers was limited. The brachytherapy dosimetry formalism should minimize the contribution of interpolation and extrapolation errors to overall dose-calculation uncertainty. Therefore, we consider the physical effects that govern the two-dimensional (2D) and one-dimensional (1D) anisotropy functions and the radial dose function, and aim to clarify the recommended approaches towards ensuring improved interpolation or extrapolation accuracy. Below are presented the rationale and recommended methods for interpolation, $r<r_{\min}$ extrapolation, and $r>r_{\max}$ extrapolation of $F(r,\theta)$, $\phi_{an}(r)$, and $g_L(r)$. Note that $r_{\min}$ and $r_{\max}$ are the smallest and largest radii for a set of reported dosimetry pa-

TABLE III. $F(r,\theta)$ for Amersham model 6733 taken directly from Sowards and Meigooni (Ref. 15).

Polar angle θ (degrees)	r [cm]						
	1	2	3	4	5	6	7
0	0.305	0.397	0.451	0.502	0.533	0.551	0.565
5	0.386	0.468	0.510	0.557	0.586	0.595	0.611
10	0.507	0.570	0.609	0.634	0.660	0.669	0.685
15	0.621	0.663	0.680	0.712	0.717	0.726	0.719
20	0.714	0.738	0.743	0.774	0.769	0.779	0.785
30	0.848	0.851	0.849	0.873	0.859	0.860	0.880
40	0.944	0.933	0.918	0.932	0.921	0.912	0.924
50	0.999	0.985	0.969	0.983	0.953	0.965	0.949
60	1.029	1.015	0.995	1.012	0.985	1.003	0.982
70	1.038	1.033	1.015	1.022	1.001	0.994	1.019
80	1.026	1.034	1.014	1.026	1.009	0.999	1.000
90	1.000	1.000	1.000	1.000	1.000	1.000	1.000
$\phi_{an}(r)$	0.967	0.964	0.953	0.966	0.953	0.948	0.955

TABLE V. $F(r,\theta)$ for Implant Sciences model 3500 taken directly from Rivard where higher resolution $\phi_{an}(r)$ data were published (Ref. 28).

Polar angle θ (degrees)	r [cm]					
	0.25	0.5	1	2	5	10
0	0.494	0.610	0.580	0.652	0.690	0.709
10	0.574	0.513	0.561	0.626	0.700	0.742
20	0.785	0.679	0.705	0.743	0.789	0.815
30	0.899	0.808	0.813	0.830	0.854	0.872
40	0.943	0.892	0.885	0.893	0.905	0.912
50	0.967	0.944	0.933	0.934	0.941	0.947
60	0.986	0.974	0.967	0.967	0.968	0.972
70	0.995	0.990	0.987	0.987	0.986	0.990
80	1.000	0.997	0.997	0.997	0.996	0.997
90	1.000	1.000	1.000	1.000	1.000	1.000
$\phi_{an}(r)$	1.164	0.973	0.933	0.931	0.938	0.948

rameters, respectively. For example, if $g(r)$ is reported for $r=\{0.5,1,2,3,4,$ and 5 cm$\}$, then $r_{\min}=0.5$ cm and $r_{\max}=5$ cm.

A. $F(r,\theta)$ 2D anisotropy function

The 2D anisotropy function is a function of polar angle for a specified radius and is normalized to unity at $\theta_0 \equiv 90°$. For all angles except θ_0, $F(r,\theta)$ values generally trend to asymptotically approach unity with increasing radial distance. The geometry function, $G(r,\theta)$, accounts for dose distribution variations attributed to distance-dependent changes in the solid angle and distribution of radioactivity, assuming a uniform radioactive distribution. Therefore, nonunity values of the 2D anisotropy function are due to nonuniform radionuclide distribution and to attenuation and scatter by the source encapsulation and internal components. As a function of polar angle, both of these effects generally change linearly over small changes in radius or angle. Dose distributions at $10° < \theta < 170°$ for 0.5-cm-long capsules are primarily affected by attenuation as a function of polar angle through the cylindrical capsule wall. Dose distributions at other angles are primarily affected by attenuation through encapsulation end welds and radiation source carriers. Away from the source long axis, $F(r,\theta)$ behavior may be considered as a combination of primary dose and dose due to photons scattered in the surrounding medium where the proportion of scattered radiation generally increases with increasing r. For the sources included in this current report and the 2004 AAPM TG-43U1 report,[2] variations in $F(r,\theta<10°)$ or $F(r,\theta>170°)$ are largely due to photon attenuation by end welds and capsule internal components. While these variations may exceed 50%, points within these volumes, i.e., $P(r,\theta<10°)$ and $P(r,\theta>170°)$, subtend ~1% of the solid-angle weighted dose rate distribution around a source. $F(r,\theta)$ may be accurately determined in general using linear interpolation. However, some sources have $F(r,\theta)$ that significantly exceed unity, e.g. the Draximage model LS-1 ^{125}I source, due to the geometry function not readily approximating the particle streaming function (i.e., *in vacuo* photon energy fluence).[10] Thus, a linear-linear interpolation method for

TABLE IV. $F(r,\theta)$ for Draximage model LS-1 taken directly from Chan, Nath, and Williamson (Ref. 24).

Polar angle θ (degrees)	r [cm]								
	0.25	0.5	0.75	1	1.5	2	3	5	10
0	3.459	1.261	0.979	0.872	0.799	0.775	0.765	0.766	0.781
10	3.312	1.246	0.977	0.877	0.808	0.787	0.775	0.778	0.786
20	2.755	1.219	0.988	0.901	0.841	0.821	0.811	0.816	0.822
30	2.130	1.178	0.994	0.925	0.877	0.861	0.854	0.864	0.873
40	1.675	1.125	0.999	0.950	0.912	0.902	0.898	0.909	0.899
50	1.380	1.073	0.998	0.967	0.945	0.938	0.934	0.940	0.935
60	1.194	1.032	0.996	0.981	0.970	0.968	0.967	0.968	0.964
70	1.085	1.007	0.998	0.994	0.990	0.989	0.988	0.991	0.993
80	1.024	0.999	1.001	1.001	0.999	0.999	0.998	1.004	0.982
90	1.000	1.000	1.000	1.000	1.000	1.000	1.000	1.000	1.000
$\phi_{an}(r)$	2.152	1.150	1.030	0.987	0.958	0.949	0.943	0.947	0.942

TABLE VI. $F(r,\theta)$ for IBt model 1251L taken from Reniers, and reprocessed using L_{eff}=4.35 mm.

Polar angle θ (degrees)	r [cm]				
	0.5	1	2	3	5
0	0.476	0.544	0.653	0.680	0.703
5	0.645	0.626	0.656	0.713	0.718
10	0.725	0.699	0.709	0.736	0.751
20	0.810	0.783	0.789	0.810	0.817
30	0.867	0.849	0.849	0.859	0.854
40	0.923	0.900	0.910	0.911	0.911
50	0.966	0.946	0.946	0.949	0.954
60	0.991	0.979	0.971	0.976	0.968
70	0.998	0.988	0.991	0.996	0.988
80	1.002	0.996	0.997	0.995	0.988
90	1.000	1.000	1.000	1.000	1.000
$\phi_{an}(r)$	1.028	0.958	0.945	0.948	0.945

TABLE VIII. $F(r,\theta)$ for Mills Biopharmaceuticals model SL-125/SH-125 taken from Li (Ref. 45) and reprocessed using L_{eff}=3.0 mm.

Polar angle θ (degrees)	r [cm]				
	1	2	3	4	5
0	0.359	0.424	0.471	0.501	0.520
10	0.429	0.493	0.535	0.563	0.574
20	0.568	0.610	0.643	0.672	0.670
30	0.710	0.744	0.759	0.771	0.762
40	0.823	0.842	0.852	0.863	0.857
50	0.918	0.926	0.936	0.937	0.921
60	0.973	0.972	0.980	0.986	0.974
70	0.985	0.987	0.989	0.993	0.993
80	0.991	1.000	1.013	1.002	0.993
90	1.000	1.000	1.000	1.000	1.000
$\phi_{an}(r)$	0.900	0.907	0.916	0.921	0.914

$F(r,\theta)$ as a function of r and θ is appropriate, and should be based on the two data points for each variable located immediately adjacent to the interpolated point of interest. This approach is identical to that recommended by the 2004 AAPM TG-43U1 report.[2]

When there is a need to extrapolate $F(r,\theta)$ data outside of the range of tabulated data, the 2004 AAPM TG-43U1 method (Appendix C 1) of using a nearest-neighbor or zeroth-order approach is still recommended since differing trends between different radionuclides do not warrant a different extrapolation methodology. Specifically, the nearest-neighbor or zeroth-order approach presented in Appendix C of the 2004 AAPM TG-43U1 report is still recommended for $F(r,\theta)$ extrapolation for $r<r_{min}$ and also for $r>r_{max}$. Regarding need for $F(r,\theta)$ extrapolation on polar angle, it appears that all sources have been characterized over the full angular range of $0°\leqslant\theta\leqslant 90°$. However, for example, if $F(7,45°)$ were sought and data were available at $F(6,40°)$ and $F(6,50°)$ data where r_{max}=6 cm, one should first perform linear interpolation to obtain $F(6,45°)$ then extrapolate (zeroth order) to obtain $F(7,45°)$.

We advise Monte Carlo dosimetry investigators to exploit continuously increasing computational and geometric modeling capabilities to estimate the dose rate distributions, including $F(r,\theta)$, as close to the source as possible and with fine angular resolution. For typical low-energy photon-emitting brachytherapy seeds which are 5 mm long and 0.8 mm in diameter capsule, it is reasonable to calculate $F(r,\theta)$ for $r\leqslant 2.5$ mm for the limited range of theta values that place calculation voxels outside of the source capsule and in the range of dose calculation points relevant to specialized clinical applications such as eye plaques.

TABLE VII. $F(r,\theta)$ for IsoAid IAI-125A taken directly from Solberg *et al.* (Ref. 36).

Polar angle θ (degrees)	r [cm]					
	0.5	1	2	3	5	7
0	0.352	0.406	0.493	0.520	0.578	0.612
5	0.411	0.465	0.545	0.584	0.658	0.701
10	0.481	0.527	0.601	0.642	0.704	0.726
20	0.699	0.719	0.757	0.775	0.794	0.799
30	0.848	0.846	0.862	0.862	0.869	0.879
40	0.948	0.936	0.932	0.916	0.937	0.969
50	1.002	0.986	0.974	0.961	0.963	0.971
60	1.029	1.024	1.008	0.993	0.990	1.001
70	1.029	1.039	1.027	1.006	1.016	1.010
80	0.999	1.025	1.024	1.023	1.009	1.025
90	1.000	1.000	1.000	1.000	1.000	1.000
$\phi_{an}(r)$	0.957	0.968	0.964	0.955	0.959	0.955

TABLE IX. $F(r,\theta)$ for Source Tech Medical model STM1251 taken directly from Kirov and Williamson erratum (Ref. 48).

Polar angle θ (degrees)	r [cm]						
	0.25	0.5	1	2	3	5	7
0	0.863	0.524	0.423	0.453	0.500	0.564	0.607
2	0.865	0.489	0.616	0.701	0.702	0.706	0.720
5	0.784	0.668	0.599	0.611	0.637	0.657	0.682
7	0.861	0.588	0.575	0.603	0.632	0.655	0.682
10	0.778	0.562	0.579	0.617	0.649	0.672	0.700
20	0.889	0.688	0.698	0.722	0.750	0.761	0.781
30	0.949	0.816	0.808	0.819	0.841	0.838	0.845
40	0.979	0.898	0.888	0.891	0.903	0.901	0.912
50	0.959	0.956	0.943	0.941	0.950	0.941	0.945
60	0.980	0.988	0.982	0.980	0.985	0.973	0.982
70	0.989	0.973	1.005	1.002	1.011	0.995	0.998
80	0.994	0.994	0.989	1.015	1.018	1.003	1.011
90	1.000	1.000	1.000	1.000	1.000	1.000	1.000
$\phi_{an}(r)$	1.210	0.982	0.942	0.937	0.947	0.938	0.944

TABLE X. $F(r,\theta)$ for Best Medical model 2335 taken from Meigooni *et al.* (Ref. 54) and reprocessed using L_{eff}=4.55 mm.

Polar angle θ (degrees)	r [cm]						
	1	2	3	4	5	6	7
0	0.797	0.690	0.674	0.672	0.663	0.675	0.630
5	0.801	0.696	0.683	0.669	0.666	0.679	0.645
10	0.790	0.690	0.673	0.675	0.665	0.690	0.644
15	0.675	0.613	0.608	0.604	0.626	0.620	0.581
20	0.608	0.591	0.596	0.601	0.616	0.647	0.595
25	0.675	0.639	0.637	0.659	0.653	0.706	0.651
30	0.681	0.660	0.679	0.694	0.694	0.717	0.672
35	0.725	0.693	0.705	0.721	0.703	0.730	0.687
40	0.762	0.736	0.750	0.747	0.741	0.775	0.720
45	0.792	0.807	0.846	0.847	0.866	0.876	0.804
50	0.885	0.880	0.885	0.887	0.909	0.907	0.835
60	0.915	0.929	0.944	0.936	0.965	1.001	0.912
70	0.932	0.960	0.972	0.965	0.975	1.014	0.916
80	0.941	0.975	0.986	0.985	0.999	1.017	0.915
90	1.000	1.000	1.000	1.000	1.000	1.000	1.000
$\phi_{an}(r)$	0.879	0.872	0.881	0.881	0.890	0.909	0.845

B. $\phi_{an}(r)$ 1D anisotropy function

The recommended $\phi_{an}(r)$ data sets were derived from solid-angle weighted dose rates based on $F(r,\theta)$ datasets, removing effects of the geometry function. These $\phi_{an}(r)$ data sets demonstrated nearly constant or linear behavior for $r \geq 1$ cm, especially for quasi mono-energetic photon sources such as ^{125}I. For $r<1$ cm, $\phi_{an}(r)$ values significantly increased with decreasing r as illustrated by Rivard, Melhus, and Kirk for a general ^{103}Pd source.[11] This behavior is caused by volume averaging of larger dose rates near the source long-axis due to the increasing ellipsoidal shape of isodose distributions in comparison to the dose rate at the same r value along the transverse plane. Based on increased availability of high-resolution $\phi_{an}(r)$ data determined over a wide range of distances, we recommend a log-linear approach to interpolating $\phi_{an}(r)$ data. The interpolation should be based on the two data points located immediately adjacent to the interpolated point of interest. This log-linear approach differs from the 2004 AAPM TG-43U1 report which previously recommended that "linear interpolation may be used to match the grid spacing of $g_X(r)$ with the grid spacing of $\phi_{an}(r)$." In light of the general behavior of $\phi_{an}(r)$ observed in multiple high-resolution datasets, it is recommended that dosimetry investigators provide sufficient spatial sampling of $\phi_{an}(r<1$ cm) and for suitably large r to minimize the need to extrapolate. This is especially convenient using Monte Carlo techniques. Additionally, having a common high-resolution sampling space for both $\phi_{an}(r)$ and $g(r)$ is crucial for implementation of the simple 1D formalism of Eq. (9) of TG-43U1.[2]

Appendix C of the 2004 AAPM TG-43U1 report recommended using Eq. (1) below, Eq. (C3) of the 2004 TG-43U1 report,[2] for extrapolating $\phi_{an}(r)$ for distances $r<r_{min}$, where r_{min} is the shortest distance for which $\phi_{an}(r)$ data are provided

$$\phi_{an}(r) \approx \frac{\phi_{an}(r_{min})}{r^2 G_L(r,\theta_0)} \quad \text{for } r < r_{min}. \tag{1}$$

In this report, we recommend replacing the aforementioned extrapolation procedure with a more accurate approach that approximates the short distance behavior of $\phi_{an}(r)$ at $r<r_{min}$ by the solid-angle (Ω) weighted integral of the line-source geometry function correction

TABLE XI. Transverse plane dose rates (cGy·h^{-1}·U^{-1}) as a function of distance for the 8 brachytherapy sources included in this report using $g_L(r)$ and $\phi_{an}(r)$, and the 1-D formalism of Eq. (11) from the 2004 AAPM TG-43U1. Results using interpolated $g_L(r)$ or $\phi_{an}(r)$ data are highlighted in **boldface** while extrapolated results based on $g_L(r)$ and/or $\phi_{an}(r)$ data are underlined.

r [cm]	Amersham EchoSeed 6733	Draximage BrachySeed LS-1	Implant Sciences 3500	IBt 1251L	IsoAid Advantage IAI-125A	MBI SL-125 SH-125	Source Tech STM1251	Best Medical 2335
0.10	7.97E+1	1.96E+1	6.56E+1	4.86E+1	7.59E+1	7.56E+1	6.48E+1	3.08E+1
0.15	4.62E+1	2.21E+1	4.17E+1	3.49E+1	4.35E+1	4.28E+1	4.16E+1	2.59E+1
0.25	1.72E+1	2.11E+1	1.67E+1	1.73E+1	1.62E+1	1.58E+1	1.73E+1	1.26E+1
0.50	4.09E+0	4.15E+0	3.93E+0	4.18E+0	3.97E+0	3.75E+0	3.99E+0	3.21E+0
0.75	1.76E+0	1.77E+0	**1.73E+0**	**1.85E+0**	1.73E+0	1.59E+0	**1.76E+0**	1.21E+0
1.0	9.48E−1	9.59E−1	9.46E−1	9.94E−1	9.50E−1	8.58E−1	9.58E−1	6.02E−1
1.5	**3.85E−1**	3.90E−1	3.94E−1	**4.15E−1**	**3.81E−1**	**3.45E−1**	**4.01E−1**	**2.00E−1**
2.0	1.95E−1	1.99E−1	2.03E−1	2.13E−1	1.90E−1	1.73E−1	2.06E−1	8.06E−2
3.0	6.85E−2	7.01E−2	7.24E−2	7.76E−2	6.40E−2	5.96E−2	7.47E−2	2.01E−2
4.0	2.95E−2	3.06E−2	3.19E−2	**3.45E−2**	**2.77E−2**	2.52E−2	**3.27E−2**	6.05E−3
5.0	1.43E−2	1.49E−2	1.57E−2	1.69E−2	1.39E−2	1.19E−2	1.60E−2	2.28E−3
6.0	7.41E−3	**7.81E−3**	8.24E−3	8.93E−3	**7.72E−3**	6.09E−3	**8.44E−3**	9.30E−4
7.0	4.12E−3	4.29E−3	4.54E−3	4.88E−3	4.37E−3	3.28E−3	4.68E−3	3.71E−4
8.0	2.28E−3	**2.43E−3**	2.59E−3	2.81E−3	2.43E−3	1.84E−3	2.67E−3	1.66E−4
9.0	1.39E−3	**1.41E−3**	1.52E−3	1.70E−3	1.64E−3	1.06E−3	1.57E−3	7.66E−5
10.0	7.92E−4	8.34E−4	9.10E−4	1.00E−3	8.49E−4	6.30E−4	9.41E−4	3.62E−5

TABLE XII. Extrapolation of $\phi_{an}(r)$ from $r=1$ cm to $r=0.25$ cm and $r=0.50$ cm. Equation (1) uses the ratio of point- and line-source geometry functions applied to $\phi_{an}(r_{min})$ to extrapolate to smaller distances. Equation (2) uses a solid-angle weighted line-source geometry function to extrapolate $\phi_{an}(r_{min})$ to smaller distances. These extrapolation approaches are tested on consensus $\phi_{an}(0.25)$, $\phi_{an}(0.50)$, and $\phi_{an}(1.00)$ data for six brachytherapy sources. The percentage error relative to the consensus $\phi_{an}(r)$ data when using Eq. (1) and Eq. (2) is indicated by $\phi_{an}(r)_{error1}$ and $\phi_{an}(r)_{error2}$, respectively. From the summary in the lower right of this table, it is apparent that $\phi_{an}(r)$ extrapolation for $r<r_{min}$ is significantly better using Eq. (2).

Source model		r [cm]	Consensus $\phi_{an}(r)$	Eq. (1)	Eq. (2)	$\phi_{an}(r)_{error1}$ [%]	$\phi_{an}(r)_{error2}$ [%]
Implant Sciences		0.25	1.164	1.078	1.160	−8.0	−0.3
3500	^{125}I	0.50	0.973	0.965	0.977	−0.9	0.4
AAPM TG-43U1S1		1.00	0.933	0.933	0.933	NA	NA
Source Tech Medical		0.25	1.210	1.089	1.172	−11.1	−3.3
STM1251	^{125}I	0.50	0.982	0.974	0.986	−0.8	0.4
AAPM TG-43U1S1		1.00	0.942	0.942	0.942	NA	NA
North American Scientific		0.25	1.288	1.128	1.241	−14.2	−3.8
MED3631-A/M	^{125}I	0.50	1.008	0.991	1.007	−1.7	−0.1
AAPM TG-43U1		1.00	0.952	0.952	0.952	NA	NA
Bebig/Theragenics		0.25	1.122	1.065	1.131	−5.3	0.8
I25.S06	^{125}I	0.50	0.968	0.966	0.977	−0.2	0.9
AAPM TG-43U1		1.00	0.939	0.939	0.939	NA	NA
Theragenics		0.25	1.130	1.015	1.119	−11.3	−1.0
200	^{125}I	0.50	0.880	0.891	0.905	1.2	2.7
AAPM TG-43U1		1.00	0.855	0.855	0.855	NA	NA
North American Scientific		0.25	1.257	1.070	1.177	−17.5	−6.8
MED3633	^{103}Pd	0.50	0.962	0.940	0.955	−2.3	−0.8
AAPM TG-43U1		1.00	0.903	0.903	0.903	NA	NA
				Average at $r=0.25$ cm		$\phi_{an}(0.25)_{error1}=-11.2\%$	$\phi_{an}(0.25)_{error2}=-2.4\%$
				Average at $r=0.50$ cm		$\phi_{an}(0.50)_{error1}=-0.8\%$	$\phi_{an}(0.50)_{error2}=0.6\%$

$$\phi_{an}(r) \approx \phi_{an}(r_{min}) \frac{\int_{4\pi} G_L(r,\theta_0)d\Omega}{\int_{4\pi} G_L(r_{min},\theta_0)d\Omega} \quad \text{for } r < r_{min}. \qquad (2)$$

When using Eq. (2) instead of Eq. (1) for sources in this report and the TG-43U1 report, extrapolating from $\phi_{an}(r_{min}=1\text{ cm})$ to $\phi_{an}(0.25)$ and $\phi_{an}(0.50)$ improved the average extrapolation accuracy by 8.8% and 0.2%, respectively, as shown comparing data at the bottom of the last two columns in Table XII. Extrapolated $\phi_{an}(r)$ values are given in Table II as used in Table XI. Care should be taken when extrapolating $\phi_{an}(r)$ to distances smaller than half the capsule length since dose rates at these distances for some polar angles are located within the source and are clinically irrelevant. For instance, for the 0.4 mm radius source capsules presented in this report, $\phi_{an}(0.10)$ was integrated over $23.6° \leqslant \theta \leqslant 156.4°$ and $\phi_{an}(0.15)$ over $15.5° \leqslant \theta \leqslant 164.5°$, both with $0.1°$ θ increments.

There were no specific recommendations given in the 2004 AAPM TG-43U1 report on how to extrapolate $\phi_{an}(r)$ at distances where $r>r_{max}$.[2] While poly-energetic sources such as ^{103}Pd exhibit significantly diminished anisotropy at distances greater than 10 cm in liquid water due to contributions from the weakly abundant high-energy photon emissions (i.e., $E\gamma \geqslant 0.3$ MeV), at this time a radionuclide-specific approach is not recommended. Conservatively, a nearest neighbor or zeroth-order extrapolation approach is recommended until more results at larger distances become available. Consequently, brachytherapy dosimetry investigators are advised to determine dose rate distributions and subsequently publish $F(r,\theta)$ and $\phi_{an}(r)$ values at distances as large as reasonably achievable. For ^{125}I and ^{103}Pd, characterization out to distances exceeding 10 cm is possible with acceptable statistical precision using modern codes. However, the investigators should limit their published results to those data where contributions from scattered radiation approximate those of an infinitely large phantom.[12,13]

C. Radial dose function

The physical effects that govern the behavior of $g(r)$ are based on attenuation and scatter in a recommended 15 cm radius liquid water medium, where broad beam attenuation is based on μ'/ρ and absorbed dose is based on μ_{en}/ρ. For points further than a few cm from the sphere surface yet beyond 1 cm for an ^{125}I or ^{103}Pd source, $g(r)$ should decrease approximately exponentially as a function of increasing r. Consequently, a log-linear function for $g(r)$ interpolation was recommended in the 2004 AAPM TG-43U1 report.[2] Upon additional examination, any logarithmic function such as $\log_{10}$ or ln (i.e., $\log_e$) will suffice to interpolate $g_L(r)$ data in a log-linear manner since differences are expressed as changes in slope and offset. Additionally, it is recommended that $g_L(r)$ data be interpolated instead of $g_P(r)$ since this latter function changes more rapidly for $r<1$ cm due to improved approximation of the particle streaming function by $G_L(r,\theta)$.[10] The log-linear interpolation should be performed using data points immediately adjacent to the radius of interest. Equation (3) may be used to solve for $g_L(r_2)$ where $r_1 < r_2 < r_3$ given $g_L(r_1)$ and $g_L(r_3)$.

$$g_L(r_2) = g_L(r_1)e^{(r_2-r_1)/(r_3-r_1)(\ln[g_L(r_3)]-\ln[g_L(r_1)])} \quad \text{for } r_1 < r_2 < r_3. \tag{3}$$

For example, if $g_L(r_1)=1.000$ and $g_L(r_3)=0.800$ where $r_1=1$ cm, $r_2=1.5$ cm, and $r_3=2.0$ cm, one may obtain $g_L(r_2)=0.894$ using Eq. (3).

Appendix C 3 of the 2004 AAPM TG-43U1 report clearly specified an extrapolation method (nearest neighbor or zeroth order) for 1D dose rate distributions when $r<r_{\min}$ for $g(r_{\min})$.[2] Due to the great variability in $g(r)$ based on choice of L and features of source construction, use of nearest-neighbor or zeroth-order data is still recommended for extrapolation of $g_L(r)$ for $r<r_{\min}$. However, the $g_P(r)$ data should then be determined by applying the ratio of the point- and line-source geometry functions to $g_L(r)$ as previously explained.

The 2004 AAPM TG-43U1 report was not explicit for extrapolating beyond $g(r_{\max})$ where $r>r_{\max}$.[2] Consequently, we have revisited the $g(r)$ extrapolation methodology, and considered a variety of fitting functions such as the bi-exponential fit as suggested by Furhang and Anderson.[14] The AAPM now recommends adoption of a single exponential function based on fitting $g_L(r)$ data points for the largest two consensus r values in a similar vein as Eq. (3). Specifically, a log-linear extrapolation as illustrated in Eq. (4) may be used to solve for $g_L(r_3)$ where $r_2=r_{\max}$, $r_1<r_2<r_3$, and given $g_L(r_1)$ and $g_L(r_2)$.

$$g_L(r_3) = g_L(r_1)e^{(r_3-r_1)/(r_2-r_1)(\ln[g_L(r_2)]-\ln[g_L(r_1)])} \quad \text{for } r_1 < r_2 < r_3. \tag{4}$$

For example, if $g_L(r_1)=0.510$ and $g_L(r_2)=0.391$ where $r_1=4$ cm, $r_2=5$ cm, and $r_3=6$ cm, one may obtain $g_L(r_3)=0.300$ using Eq. (4). Using $g_L(r_{\max})$ as a test for extrapolating $g_L(r)$ data for the sources included in this report, the single exponential function extrapolation technique reduces $g_L(r)$ extrapolation errors by over 40% as compared to zeroth-order extrapolation, with negligible differences in comparison to more complex fits such as a three-point linear regression. Therefore, the AAPM recommends that treatment planning software manufacturers no longer employ a zeroth-order approach for determining $g_L(r)$ extrapolated values beyond $g_L(r_{\max})$, and that they immediately use a single exponential fit to extrapolate $g_L(r)$ values based on the furthest two consensus data points. Following this guidance, Table II includes $g_L(r)$ and $g_P(r)$ extrapolated beyond $r_{\max}$ for the sources included in this report.

To provide practical data for treatment planning quality assurance that typically uses $g_P(r)$ instead of $g_L(r)$, values in Table XI include extrapolated $\phi_{an}(r)$ or $g_P(r)$ data. These latter data were converted from extrapolated $g_L(r)$ data since $g_P(r)$ changes more rapidly and may be derived from $g_L(r)$ using the ratio of the point- and line-source geometry functions. It is also noteworthy to point out that these interpolation and extrapolation techniques may be extended to the dosimetry parameters in the 2004 AAPM TG-43U1 report or other brachytherapy sources in general.

IV. SUMMARY

As stated in the AAPM TG-43U1 report, the AAPM recommends that the revised dose-calculation protocol and revised source-specific dose-rate distributions be adopted by all end users for clinical treatment planning of low-energy brachytherapy using interstitial sources. Depending upon the dose-calculation protocol and parameters currently used by individual physicists, adoption of this protocol may result in changes to patient dose calculations. These changes should be carefully evaluated and reviewed with the radiation oncologist preceding implementation of the current protocol.

ACKNOWLEDGMENTS

The authors wish to thank Frank A. Ibbott for creation of the artwork in Fig. 1, which was supported by the AAPM Therapy Physics Committee (TPC). Also, we extend our appreciation to Sujat Suthankar of Rosses Medical Systems (now at Implant Sciences) for discussions on Sec. III. Furthermore, we thank Janelle A. Molloy for AAPM TPC review and Zuofeng Li, Ning J. Yue, and Bruce Thomadsen of the AAPM BTSC for their constructive comments and careful review of this report. We also wish to thank David W. O. Rogers for bringing the air mass density correction to our attention. Some of the authors (M.J.R.; A.S.M.; R.N.; J.F.W.) have received research support to perform dosimetry studies for the sources included herein (Implant Sciences Corp., Mills Biopharmaceuticals Corp.; International Brachytherapy, IsoAid Corp., and Best Medical Inc.; DraxImage Inc.; DraxImage Inc. and SourceTech Medical, respectively).

APPENDIX: MODEL-SPECIFIC SOURCE DOSIMETRY DATA

The following sections summarize the dosimetry parameters for each source, listed alphabetically. A description of the source and its references are first provided. Afterwards each dosimetry parameter is discussed briefly.

A. Amersham model 6733 ^{125}I source

The EchoSeed™ model 6733 source was introduced in 2001, and is similar to the model 6711 source. The model 6733 consists of a 4.5 mm welded titanium capsule with its external surface having several circular grooves, 0.8 mm in diameter, and a titanium wall 0.05 mm thick, with welded end caps. The grooves are to enhance the ultrasound visualization of the sources. The capsule contains a 3.0-mm-long, 0.5-mm-diam silver rod onto which ^{125}I is adsorbed. (Fig. 1). The active length for the geometry function line-source approximation is $L=3.0$ mm.

There are two published papers for this model; one dealing with Monte Carlo determination by Sowards and Meigooni,[15] and the other by Meigooni *et al.* dealing with experimental dose determinations using TLDs.[16] Both of these papers report values for all the TG-43 parameters. The Monte Carlo calculations were performed both in SolidWater™ (model 457 by Radiation Measurements Inc., of Middletown, WI) and in liquid water, and used the PTRAN

version 7.43 Monte Carlo code. Photon cross sections used were from DLC-99 with mass energy absorption coefficients from Hubbell and Seltzer.[17] Experimental results were obtained using TLD-100 chip dosimeters (Harshaw/Bicron of Solon, OH) in a SolidWater™ phantom. The calibration of the TLD chips was performed using a 6 MV beam and an energy correction factor of 1.4 was used. Correction from SolidWater™ to water was done with a factor of 1.05 borrowed from Williamson.[18] The standard deviation from 16 chips was 5%. These measurements in SolidWater™ were compared with measurements by Meigooni *et al.* in SolidWater™.[16]

1. 6733 Λ

Values for the Monte Carlo dose rate constant were obtained at a point on the transverse plane in both liquid water and SolidWater™. Using the liquid water results, ${}_{MC}\Lambda = 0.99$ cGy h^{-1} U^{-1}. The air-kerma strength was measured at NIST in Spring 2001 with ${}_{EXP}\Lambda$ measured in SolidWater™ using TLDs. After correction to liquid water, the value of ${}_{EXP}\Lambda$ was 0.97 cGy h^{-1} U^{-1}. Averaging these values gives a ${}_{CON}\Lambda = 0.98$ cGy h^{-1} U^{-1} as in Table I.

2. 6733 $g(r)$

The Monte Carlo and measured values for $r \geq 1$ cm for the radial dose function agree within 5%, which is within the experimental uncertainties. Therefore, Table II shows ${}_{CON}g(r)$ as taken from the Monte Carlo data set in liquid water.

3. 6733 $F(r,\theta)$

Experimental and Monte Carlo results agree within 5% for angles greater than 20°. The experimental and Monte Carlo results agree within 5% for distances 5 cm or greater, but have greater differences at 0° for a distance of 2 cm because of uncertainties in the TLD measurement. Table III presents the consensus model 6733 $F(r,\theta)$ data taken directly from Sowards and Meigooni.[15]

B. Draximage model LS-1 ^{125}I source

The BrachySeed™ model LS-1 source was approved by the U.S. Food and Drug Administration in October 2000 and introduced to the North American market in 2001 by Cytogen Corporation (Princeton, NJ), under license from DRAXIS Health Inc. (Mississauga, Ontario, Canada). The BrachySeed™ was distributed by Draximage Inc. (Kirkland, Quebec, Canada), a subsidiary of DRAXIS Health Inc. Production stopped in February 2006, but these data are of interest to dosimetry investigators and interpretation of clinical trial results.

The model LS-1 features a two-bead geometry and unique laser weld about the center of the 4.4-mm-long and 0.8-mm-diam seed. ^{125}I is uniformly impregnated in 0.5 mm diameter ceramic (alumina-silicate) beads, separated by a 2.97-mm-long Pt/Ir radio-opaque marker (Fig. 1). A medial Ti spacer is included to center the x-ray marker and provide a surface for the central weld of the two end capsules, which have a wall thickness of 0.05 mm. There are four peer-reviewed papers that assess the 2D dosimetry parameters of the BrachySeed™ model LS-1, and a fifth publication describes a consensus dataset methodology using the BrachySeed™ publications as examples.

Nath and Yue measured 2D brachytherapy dosimetry parameters in a water-equivalent phantom using 1 mm^3 TLD rods and TLD-specific calibration factors.[19] A SolidWater™ to liquid water correction factor of 1.043 obtained by Williamson[18] and a TLD energy dependence correction of 1.41 published by Meigooni *et al.*[20] were used to calculate Λ. On the transverse plane, radial distances are listed for a range of 0.5–7 cm, and 2D measurements are reported between 1 and 6 cm. A correction was made to account for the 1999 NIST WAFAC anomaly, which impacted measurements of Λ by +6.8%. Towards the calculation of 2D dose distributions, results were presented for both a line source model ($L_{\text{eff}} = 4.1$ mm) and a two-point source model (separation = 3.6 mm).

Chan and Prestwich measured and calculated dosimetry parameters for the model LS-1 source.[21] Measurements were performed using GafChromic MD-55-2 film, which is currently not a well-established method for determining single-seed brachytherapy dose distributions, and the data were not included in the consensus. Chan and Prestwich used the Integrated Tiger Series CYLTRAN (version 3.0) with photon cross sections published by NIST[17] to perform Monte Carlo photon transport simulations. The CYLTRAN code has been benchmarked using the MED3631-A/M ^{125}I source. The authors state that the source geometry was modeled exactly with the exception of the capsule ends, which were given a flat thickness of 60 μm instead of modeling a spherical shell with thickness 65 μm. s_K was estimated using a cylindrical volume of air and a 5 keV photon energy cutoff to simulate the NIST WAFAC. Material densities and compositions were not explicitly stated, and the calculation geometry was described as a series of concentric cylinders. A two-point source model with 3.6 mm separation was employed for reconstructing 2D brachytherapy dose distributions. The number of particle histories was chosen to ensure that 1 σ standard uncertainty about the mean was less than 1%.

Williamson[22] published calculated single-seed brachytherapy dosimetry parameters for the model LS-1 ^{125}I seed using the PTRAN code (PTRAN_CCG, version 7.43), the DLC-146 photon cross-section library, and the mass-energy absorption coefficients of Hubbell and Seltzer.[17] The collision kerma rate at a given geometric location was calculated using the bounded next flight estimator, and for distances less than 3 mm, a once-more collided flux point-estimator was employed. Results for $g(r)$ were evaluated over 0.1–14 cm in radial distance. $F(r,\theta)$ was evaluated from 0.25 to 10 cm in distance range and over $0° \leq \theta \leq 180°$ at 34 angular increments with a maximum 5° spacing, although, data were presented graphically. Towards calculation of Λ, S_K was estimated by simulating the measurement geometry of the NIST WAFAC. Ti characteristic x-ray production was

suppressed in the PTRAN code to simulate the function of the aluminum filter in the NIST WAFAC. Three geometry functions were included in the 2D dosimetry calculations: a point source model, a two-point source model (separation =3.6 mm), and a line source model of length 7.2 mm. Additional simulations were performed to assess the variation of $g(r)$ with respect to internal motion of the active beads. The number of starting particles was chosen to provide statistical standard errors of the mean between 0.2% and 2%.

For the BrachySeed™ model LS-1 ^{125}I source, Wang and Sloboda[23] calculated the 2D dosimetry parameters using EGS4 and an associated user code, DOSCGC. A track-length estimator was used to score photon energy fluence and then combined with appropriate mass-energy absorption coefficients from Hubbell and Seltzer to estimate absorbed dose. Furthermore, the EGS4/DOSCGC code was verified by the authors using the model 6702 and 6711 ^{125}I brachytherapy seeds, among other radiation sources. As EGS4 does not simulate the production of characteristic x rays, three methods were used to model characteristic x-ray production from the Ag doped into the ceramic beads. Published results of Wang and Sloboda include the method that simulates characteristic x-ray production by determining the probability of interaction between the principal ^{125}I photons and Ag.[23] Results were evaluated between 0.1 and 14 cm of radial distance for $g(r)$ and over 0.25–10 cm for $F(r,\theta)$ using a spherical coordinate geometry. Ti characteristic x-ray contributions were removed to simulate NIST WAFAC measurement. Assuming a source separation of 3.6 mm, a double-point model was used in the reconstruction of the 2D dose distributions.

Chan, Nath, and Williamson[24] published a methodology for constructing consensus reference dosimetry parameters for a single brachytherapy source, and used the four aforementioned BrachySeed™ publications as an example. Additionally, Chan, Nath, and Williamson included minor corrections or clarifications of results published by Chan and Prestwich and by Williamson,[22] and a detailed table of Williamson's $F(r,\theta)$ data is included, which was not present in the original publication. The recommended consensus values in Chan and co-workers[24] are similar to those published here, with specific differences listed below. However, the 1D dose rate per unit air-kerma strength values published in Table IV of Chan *et al.* are not in agreement with the recommended dosimetry data of Chan *et al.*[24] For example, a value of 0.9673 cGy $h^{-1}\cdot U^{-1}$ is published for 1 cm, while a value of 0.9594 cGy $h^{-1}\cdot U^{-1}$ is expected ($_{\mathrm{CON}}\Lambda=0.972$ cGy $h^{-1}\cdot U^{-1}$; $\phi_{an}(r)=0.987$; and, $g_P(r)=1$). Because of this discrepancy and because Chan *et al.* do not describe how the values were generated, use of the 1D dose rate per unit air-kerma strength values in Table IV of Chan *et al.*[24] to validate the entry of consensus dosimetry data into a given treatment planning system is not recommended.

1. LS-1 Λ

Nath and Yue[19] published a measured Λ value of 1.02 ± 0.07 cGy $h^{-1}\cdot U^{-1}$ that includes correction for the 1999 NIST WAFAC anomaly using TLDs in a SolidWater™ phantom. The GafChromic film measurement of Chan and Prestwich[21] yielded 0.98 ± 0.06 cGy $h^{-1}\cdot U^{-1}$, but is not included in the $_{\mathrm{CON}}\Lambda$ derivation since radiochromic film is still considered an experimental method for determining low-energy photon dosimetry characteristics. Thus, $_{\mathrm{EXP}}\Lambda$ is 1.02 cGy $h^{-1}\cdot U^{-1}$. Chan and Prestwich published[21] $\Lambda=0.90\pm0.03$ cGy $h^{-1}\cdot U^{-1}$ using the CYLTRAN code, but updated the value in Chan *et al.*[24] after improved source modeling to be $\Lambda=0.918$ cGy $h^{-1}\cdot U^{-1}$.[24] Williamson[22] published $\Lambda=0.935$ cGy $h^{-1}\cdot U^{-1}$ using the PTRAN code and the WAFAC geometry for solid-angle averaging, and Wang and Sloboda[23] published $\Lambda=0.932\pm0.003$ cGy $h^{-1}\cdot U^{-1}$ using EGS4 at a point on the transverse plane. Consequently, $_{\mathrm{MC}}\Lambda=0.928$ cGy $h^{-1}\cdot U^{-1}$ was obtained, and $_{\mathrm{CON}}\Lambda=0.972$ cGy $h^{-1}\cdot U^{-1}$ (Table I).

2. LS-1 $g(r)$

The Monte Carlo results of Williamson[22] and of Wang and Sloboda[23] covered the largest radial distance range and came closest to the source. After both datasets were converted to a common effective length of 4.1 mm, agreement in $g_L(r)$ between the two reports was <2% within 5 cm, increases to 6% at 10 cm, and is 10% at 14 cm. Because the Williamson[22] result included greater sampling at large radial distances, the $g(r)$ results generated using PTRAN are recommended for $_{\mathrm{CON}}g(r)$ data (Table II). Note that the experimental data of Nath and Yue[19] and the Monte Carlo result of Chan and Prestwich,[21] corrected to $L_{\mathrm{eff}}=4.1$ mm, were also in good agreement, often within 5%. The publication by Williamson[22] contains a rounding error in its Table III, where the $g(r)$ values *listed* at 0.8 cm were actually *calculated* for a radial distance of 0.75 cm.[25] This error was corrected in Chan, Nath, and Williamson[24] by publishing data at a radial distance of 0.8 cm, although, Chan *et al.* do not acknowledge the error or publication of new data. The corrected value for 0.75 cm is included in $_{\mathrm{CON}}g(r)$.

3. LS-1 $F(r,\theta)$

Monte Carlo results of Williamson,[22] published in Chan, Nath, and Williamson[24] were chosen to be the consensus $F(r,\theta)$ dataset because they featured finer radial distance range resolution below 2 cm and higher angular resolution near $\theta=0°$ and $\theta=90°$ compared to that of Wang and Sloboda.[23] The data were compared with Monte Carlo results by Chan and Prestwich,[21] and with TLD results by Nath and Yue[19] at common radial distances of 1, 2, and 5 cm. Over these radii, the Chan and Prestwich[21] results agreed with Williamson's[22] data within ±2% [maximum was −8.5% at $F(5,0°)$]. Nath and Yue results were generally +6% in comparison to those by Williamson,[22] with a maximum difference of +11.5% at (5,50°).

Towards derivation of $_{\mathrm{CON}}F(r,\theta)$, Williamson's[22] high-angular resolution data were condensed using the recommendations of TG-43U1 (Sec. V Part B.4) to simplify entry into treatment planning systems, and results taken directly from Chan, Nath, and Williamson[24] in Table IV are presented us-

ing a 10° sampling space. Calculation of $\phi_{an}(r)$ using the condensed ${}_{\mathrm{CON}}F(r,\theta)$ data yields results within 0.1% of Williamson's,[22] except at 0.25 cm where the discrepancy is −1.3%; thus the $\phi_{an}(r)$ data from Williamson in Chan and co-workers[24] are used herein.

C. Implant Sciences model 3500 ^{125}I source

The model 3500 I-Plant™ source was first marketed in August 2000 and is notable for a novel manufacturing process involving ion implantation with ^{124}Xe. The outer surface of a 0.64-mm-diam quartz tube is coated with a 16 μm layer of silicon into which approximately 10^{17} ^{124}Xe ions are implanted. A 5-μm-thick layer of SiO_2 is then applied as an overcoat to contain the xenon and later the radioactive ^{125}I. These nonradioactive-doped quartz tubes are then stored until ^{125}I seeds are needed. At that time, the ^{125}Xe is neutron activated to ^{125}I, and the assembly, consisting of the quartz tube and a conical ended silver radiographic marker inside the tube, is sealed in a laser-welded titanium capsule. Fig. 1 illustrates the assembled source. The wall thickness of the 0.8-mm-diam titanium capsule is 0.05 mm, and the end welds are 0.25 mm thick. The overall seed length is 4.5 mm, and the effective active source length, L_{eff}, is taken as the length of the glass tube, 3.76 mm.

Four published papers were reviewed to determine the full consensus dataset for the model 3500 I-Plant™ source. Duggan and Johnson[26] measured dosimetry parameters using LiF TLD rods in SolidWater™ for dose rate constant measurements and in PlasticWater™ (CIRS PW2030) for radial dose function and anisotropy measurements. The TLDs were calibrated against ^{60}Co, and the distance-dependent phantom to water correction was calculated from the MCNP4B Monte Carlo code based on the NIST measured photon spectrum of the model 3500 source. The PlasticWater™ to liquid water correction varied from 0.99 at 0.5 cm to 1.07 at 7 cm. Three separate measurements of the dose rate constant, each measurement based on six TLD rods, were made, but the actual determination was by cross calibration relative to Accredited Dosimetry Calibration Laboratory (ADCL) calibrated Amersham model 6711 seeds. Radial dose function measurements were made at 0.5 cm increments from 0.5 to 5.0 cm and at 6.0 and 7.0 cm. Anisotropy was measured at 9 or 10 angles in a given quadrant at distances from 1–4 cm in 0.5 cm increments and at 5, 6, and 7 cm.

Wallace[27] also determined dosimetry parameters, and used LiF TLD rods in plastic water phantoms (CIRS PW2030) measuring $30\times30\times7$ cm^3. The TLDs were calibrated against ^{60}Co, and corrections for the plastic phantom, finite TLD volume, and energy response were applied to the TLD readings. Twelve evaluations of the dose rate constant, each based on ten TLD rods at 1 cm from one of two seeds with NIST traceable calibrations, were made with an estimated net uncertainty of 6% ($k=2$). Wallace measured the radial dose function at 0.5 cm increments from 0.5 to 6.0 cm and at 1.0 cm increments from 7.0 to 10.0 cm plus some intermediate distances.[27] Two-dimensional anisotropy was measured in 10° increments from 0° to 90° at distances from 1 to 6 cm in 1.0 cm increments and at 0.5, 0.75, and 1.5 cm. With at most 3.5 cm of top/bottom scattering material, these results may be lower than expected values by at least a few percent due to differences from an infinite scattering environment. Therefore, these data are not recommended.

Two papers reported Monte Carlo calculated dosimetry parameters for this source. Rivard[28] also used the MCNP4B software and photon and electron cross sections from the supplied DLC-189 library with the source in a 30-cm-diam phantom. Dose rates were calculated from the MCNP pulse height tally, and the dose rates extrapolated to zero distance (to remove effects of air attenuation) after subtraction of titanium fluorescent x-ray contributions to calculate the dose rate constant. Each calculation of Λ, $g(r)$, and $F(r,\theta)$ involved 2×10^9 photon histories. The radial dose function was calculated at distances from 0.05 to 10 cm with a standard deviation typically less than 0.3%. Two-dimensional anisotropy function was reported in 5° increments from 0° to 90° at distances from 0.05 to 10 cm. The statistical uncertainty in these calculations was angle dependent, ranging from $<$0.3% at 90° to 3% at 0°.

While the Monte Carlo calculations by Duggan[29] also used MCNP to calculate the radial dose function of the model 3500 source, the impact of using versions 4C2 and 5 was examined. The latter version includes completely revised low-energy photon cross-section data. Each simulation consisted of four-batches of 3×10^8 histories. Using an effective source length, $L=4$ mm, the radial dose function was calculated at distances from 0.25 to 10 cm with a standard deviation $\leqslant$0.3% in the range 0.5–8 cm.

1. 3500 Λ

Because Duggan and Johnson[26] used a relative methodology comparing the air-kerma strength adjusted dose rates of the model 3500 with that of a measured Amersham model 6711 source, their value of Λ was not included in the average of ${}_{\mathrm{EXP}}\Lambda$. The Wallace[27] value of the dose rate constant in water, 1.01 ± 0.005 cGy h^{-1} U^{-1}, was taken as ${}_{\mathrm{EXP}}\Lambda$. The MCNP derived value of the dose rate constant from Rivard[28] of 1.017 ± 0.04 cGy h^{-1} U^{-1}, obtained by extrapolating to zero distance on the transverse plane, was taken as ${}_{\mathrm{MC}}\Lambda$. Averaging these two values gives a ${}_{\mathrm{CON}}\Lambda$ of 1.014 cGy h^{-1} U^{-1} as in Table I.

2. 3500 $g(r)$

The Monte Carlo values of $g(r)$ from Duggan[29] in the range 0.5–10 cm were converted to $L_{\mathrm{eff}}=3.76$ mm and are listed as ${}_{\mathrm{CON}}\Lambda g(r)$ in Table II. These values were chosen because the updated low-energy photon cross sections used by Duggan[29] are considered more accurate than those used by Rivard,[28] particularly at greater distances. Values at $r<0.5$ cm from the source, where differences in the photoelectric interaction cross sections are less important, are taken from Rivard.[28]

3. 3500 $F(r,\theta)$

Comparing $F(r,\theta)$ at the common radial distances of 1, 2, and 5 cm, the average pair wise difference between the three published values is less than 6%. The maximum difference is 24.8% between the Monte Carlo results and Wallace's[27] values at $F(1,10°)$. The maximum difference between the two TLD studies is 14.5% at $F(5,20°)$. Because the MCNP-derived values of $F(r,\theta)$ from Rivard[28] are of finer angular resolution and finer distance resolution less than 2 cm from the source than those of the TLD based measurements,[26,27] these are chosen as ${}_{\mathrm{CON}}F(r,\theta)$ in Table V.

D. IBt model 1251L ^{125}I source

A double walled encapsulated source of radioactive ^{125}I was developed in 2000 for interstitial brachytherapy by International Brachytherapy (IBt, SA Zone Industrielle C, Seneffe, Belgium 7180). The source is marketed as InterSource[125] model 1251L and is composed of two concentric titanium tubes of 0.04 mm wall thickness, laser welded at the edges (Fig. 1). The capsule diameter is 0.8 mm, and capsule length is 4.5 mm. An x-ray marker composed of 0.045-mm-thick 90% platinum/10% iridium alloy is attached to the inner tube. The radioactive iodine is deposited on the inner tube in three printed bands. The distance between the outermost edges of the bands of activity is 3.7 mm. The sources are available with air-kerma strengths between 0.254 U and 1.27 U. The source strength is determined by comparison to the NIST WAFAC standard, developed in 1999 and revised in 2000. The lack of silver in this design results in dosimetric characteristics that are very different from those of the Amersham model 6711 seed, and similar designs that incorporate silver. Instead, the dosimetry data are more consistent with those of the Amersham model 6702 seed, which likewise did not incorporate silver.[2]

Dosimetry characteristics have been reported for this source model by Reniers, Vynckier, and Scalliet[30,31] and by Meigooni *et al.*[32] Both reports were based on the revised 1999 NIST standard. Both authors performed measurements in a solid water-equivalent phantom with 1 mm^3 LiF thermoluminescent dosimeters. Reniers *et al.* used material identified as "WT1" without further description. Meigooni used SolidWater™. The TLDs were calibrated in a 6 MV accelerator beam by both authors. Reniers used an energy correction factor of 1.41 while Meigooni *et al.* reported using a value of 1.4. Neither author adjusted the energy conversion factor with distance from the source. Reniers, Vynckier, and Scalliet[30] performed Monte Carlo calculations using the MCNP4B code, with antiquated photoelectric cross-section libraries. Those calculations were later updated by Reniers, Vynckier, and Scalliet[31] using the more recent cross-section data from EPDL97 and from XCOM. Meigooni used PTRAN v.6.3 Monte Carlo code with the DLC-99 cross-section libraries.[32] Both authors performed calculations to estimate the dose in water-equivalent plastic for comparison with measurements. Additional calculations were performed with liquid water as the medium.

1. 1251L Λ

Reniers, Vynckier, and Scalliet[30] measured a dose rate constant in WT1 of 1.03±0.07 cGy h^{-1} U^{-1}, and calculated a corresponding value of 0.98±0.01 cGy h^{-1} U^{-1} (where the uncertainty of the Monte Carlo calculations is a reflection of the statistical uncertainty only). They then calculated the dose rate constant in water to be 1.02±0.01 cGy h^{-1} U^{-1}, obtained at a distance of 5 cm on the transverse plane. Reniers and co-workers used the ratio of calculated values to determine a correction factor for WT1.[30] They reported a value of 1.031, although the ratio is in fact 1.041. The plastic-to-water correction factor was then applied to the TLD measurements to estimate a measured value of dose rate constant in water of 1.072 cGy h^{-1} U^{-1}, although Reniers and co-workers reported this value to be 1.05±0.07 cGy h^{-1} U^{-1}.[30]

Meigooni *et al.* reported a measured dose rate constant in SolidWater™ of 1.014±0.08 cGy h^{-1} U^{-1}.[32] They also calculated a value of 0.981±0.03 cGy h^{-1} U^{-1}, obtained at 5 cm by extrapolating to 1 cm on the transverse-plane. The calculated dose rate constant in water medium was 1.013±0.03 cGy h^{-1} U^{-1}. Calculated dose rate constants from Meigooni *et al.* can be used to determine a correction factor for SolidWater™ of 1.033, leading to an estimated measured value in liquid water of 1.047 cGy h^{-1} U^{-1}, although Meigooni *et al.* did not report this value.[32] Measured and calculated values from both publications have been averaged to yield ${}_{\mathrm{CON}}\Lambda = 1.038$ cGy h^{-1} U^{-1}.

2. 1251L $g(r)$

All three publications[30–32] considered the active length of the source to be the distance between the outermost edges of the bands of activity, or 3.7 mm. Recently, the AAPM recommended a value of 4.35 mm,[6] which has been used here to assure consistency among data sets. The data from Meigooni *et al.*[32] were selected to represent the consensus data due to the smaller range of the Reniers *et al.* data and the use by Reniers *et al.* of outdated cross-section libraries in their first publication.[30] In addition, the data from Meigooni *et al.* and the recalculated data from Reniers *et al.* from the second publication are in very close agreement.[31] Monte Carlo calculations by Meigooni *et al.* showed better agreement with their measured data in comparison to the diminished internal consistency of the first paper from Reniers *et al.* calculations and measurements. This inconsistency in the Reniers *et al.* data has been resolved in their next publication.[31,33] Thus, the data of Meigooni *et al.* were recalculated using L_{eff}=4.35 mm and presented in Table II.

3. 1251L $F(r,\theta)$

Reniers and co-workers[30] and Meigooni *et al.*[32] performed measurements and calculations of anisotropy function. Measurements by Reniers and co-workers[30] were made in WT1 at 2, 3, and 5 cm, at increments of 10° around the source, and corresponding calculations were performed for comparison. Calculations were performed in liquid water medium at

0.5, 1, 2, 3, and 5 cm from the source, at increments of 5°. TLD measurements of anisotropy by Meigooni *et al.*[32] were made in SolidWater™ at 2, 3, 5, and 7 cm, with 10° increments, and calculations were made at 2, 3, and 5 cm for comparison. Meigooni *et al.* also performed calculations in liquid water medium from 1 to 7 cm from the source in 1 cm increments and from 0° to 90° and with 10° increments. Monte Carlo calculations from Reniers and co-workers,[30] reprocessed using L_{eff}=4.35 mm, were chosen for ${}_{\text{CON}}F(r,\theta)$ (Table VI) because of their consistency with measurements from Meigooni *et al.*[32] and Reniers and co-workers.[30] Monte Carlo calculations by Meigooni *et al.*[32] show nonphysical excursions at θ=0°, and values considerably greater than unity at angles close to 90°.

E. IsoAid model IAI-125A ^{125}I source

The IsoAid ADVANTAGE™ ^{125}I model IAI-125A source was introduced in the North American market in 2002. The model consists of a cylindrical silver core, 3 mm long and 0.5 mm in diameter, onto which ^{125}I has been uniformly adsorbed as a 1-μm-thick coating of silver halide. The silver core is sealed within cylindrical titanium housing with a physical length of 4.5 mm and outer diameter of 0.8 mm (Fig. 1). The cylindrical portion of the titanium housing is 0.05 mm thick, with rounded titanium welds at each end. There are two published papers for this model; both of these papers report values for all the TG-43 parameters.[34–36]

In 2002, Meigooni *et al.* published the results of both TLD measurements and Monte Carlo simulations of the dosimetric characteristics of the model IAI-125A source.[34,35] The measurements were performed in a SolidWater™ phantom of dimension ($25\times25\times20$ cm^3), machined precisely to accept LiF TLD-100 chips of dimensions ($3.1\times3.1\times0.8$ mm^3) and ($1.0\times1.0\times1.0$mm^3). An energy response correction factor between the 6 MV calibration energy and ^{125}I of 1.4 was used.[37] Nonlinearity correction of the TLD response for the given dose was included. Monte Carlo simulations utilized the PTRAN code in both SolidWater™ and water. Although unspecified, it was learned that the DLC-99 photon cross section library was employed. Simulation data from 1.375×10^6 histories (divided into 55 batches) were combined using a distance and attenuation-average bounded next flight point kerma estimator.[38] This resulted in standard errors about the mean ranging from 1.5% (near the source: $r<3$ cm) to 5–6% (far from the source: $r>5$ cm). s_K was determined by calculating the air-kerma rate at a distance of 5 cm and subsequently correcting for inverse square law to 1 cm. The titanium characteristic x-ray production was suppressed for the simulations of air-kerma rate in air.

Solberg *et al.*[36] published the results of Monte Carlo calculations and TLD measurements on the model IAI-125A source in 2002. The measurements were performed in a Plastic Water® phantom (model PW2030, Computerized Imaging References Systems of Norfolk, Virginia) of dimensions ($30\times30\times7$ cm^3), machined precisely to accept LiF TLD-100 rods of dimensions 6 mm long and 1 mm diameter. A correction factor of 0.995, calculated for the phantom material at 1 cm, was applied to TLD responses to arrive at the dose rate constant in water. The IAI-125A source, used for measurements, had a direct traceability to NIST (1999 standard). Total combined uncertainty of dose rate constant measurement was estimated at 4.8%. The component uncertainties that contribute to the combined uncertainty are an assumed uncertainty of 0.5% for the air-kerma strength S_K, statistical uncertainty in the TLD responses of 4–5%, uncertainty in the TLD energy correction factor of 1–2%, and a phantom correction of 2%. These uncertainties were added in quadrature to arrive at the combined estimated uncertainty of 4.8%. The radial dose function had a quoted uncertainty of 7–8% at the 95% confidence level and the net uncertainty of the anisotropy data was quoted at 10% which results from statistical uncertainty of the measurements of TLD responses. As above for the model 3500 ^{125}I source for consistency, these data were excluded due to lack of sufficient backscattering material and these data are not recommended. Monte Carlo simulations utilized the MCNP4C in liquid water. The photoelectric cross section data were taken from XCOM tabulations of Berger and Hubbell.[39] The ^{125}I spectrum used for all calculations consisted of five energies which were similar to those recommended in AAPM TG-43U1.[2] Dose rate was determined at 1 cm in a cylindrical annulus 0.05 cm thick$\times$0.05 cm deep. The MCNP *F4 tally was used to score the energy fluence in the cylindrical annulus; the energy fluence was converted to dose rate using mass-energy absorption coefficients obtained from Seltzer.[40] Air-kerma strength was scored in vacuum in a similar cylindrical geometry 0.2 cm thick$\times$0.2 cm deep at a radial distance of 50 cm from the center of the source. For TLD measurements, the geometry function was calculated using the AAPM TG-43 approximation for a line source; for Monte Carlo calculations, MCNP was used to determine the particle streaming function.[10,41–43]

1. IsoAid IAI-125A Λ

Meigooni *et al.* published a measured Λ value of 1.02 ± 0.08 cGy $h^{-1}\cdot U^{-1}$;[34,35] this was obtained by multiplying the TLD measured dose rate constant (0.99) by the ratio (0.98/0.95) of the Monte Carlo simulated dose rate constant in water to SolidWater™. Solberg *et al.* published a measured value of $\Lambda=0.96\pm0.05$ cGy $h^{-1}\cdot U^{-1}$.[36] Thus, ${}_{\text{EXP}}\Lambda=0.99$ cGy $h^{-1}\cdot U^{-1}$. Meigooni *et al.* published $\Lambda=0.98\pm0.03$ cGy $h^{-1}\cdot U^{-1}$ in water using the PTRAN code obtained at 5 cm by extrapolating to 1 cm on the transverse plane.[34,35] Solberg *et al.* published $\Lambda=0.962\pm0.005$ cGy $h^{-1}\cdot U^{-1}$, using the MCNP code.[36] Here, air-kerma strength was determined at 50 cm on the transverse plane with vacuum between the source and tally region. Consequently, ${}_{\text{MC}}\Lambda=0.971$ cGy $h^{-1}\cdot U^{-1}$ was obtained as an average of these two results, and ${}_{\text{CON}}\Lambda=0.981$ cGy $h^{-1}\cdot U^{-1}$ as shown in Table I.

2. IsoAid IAI-125A $g(r)$

Both Meigooni *et al.*[34] and Solberg *et al.*[36] obtained $g_L(r)$ data using measurements and calculations. The ratio of Mei-

gooni *et al.* corrected measurements and calculations for liquid water from $r=0.5$ to 6.0 cm was typically 0.95, and ranged from 0.99 at 0.5 cm to 0.87 at 5.0 cm. Over the same radial range, the ratios were typically 0.98 for Solberg *et al.*,[36] and ranged from 0.96 at 3.0 cm and 1.02 at 6.0 cm. Comparisons of Monte Carlo results by Meigooni *et al.*[34] and Solberg *et al.*[36] gave an average ratio of 1.06 from 0.5 to 6.0 cm, ranging from 0.97 at 0.5 cm and 1.12 at 4.0 cm. Comparisons of TLD results by Meigooni *et al.*[34] and Solberg *et al.*[36] gave an average ratio of 0.98 over the same radial range, and ranged from 1.03 at 1.5 and 0.93 at 5.0 cm. Based on this analysis, there was good agreement among the calculations of Solberg *et al.*,[36] measurements by Solberg *et al.*,[36] and measurements by Meigooni *et al.*[34] Thus, the Monte Carlo results of $g_L(r)$ directly from the publication by Solberg *et al.*[36] were chosen as the consensus data set and listed in Table II, with italicized data indicating data from Meigooni *et al.*[34] to expand the radial range.

3. IsoAid IAI-125A $F(r,\theta)$

Meigooni *et al.*[34] calculated results using an end weld thickness of 0.1 mm, while Solberg *et al.*[36] calculated using 0.25 mm. Thus, it was expected that the anisotropy along the long axis would be larger as calculated by Solberg *et al.*[36] in comparison to Meigooni *et al.*[34] Solberg *et al.*[36] also explicitly mentioned that the source geometry was per manufacturer provided specifications. Finally, results of Meigooni *et al.*[34] exhibited nonphysical behavior of anisotropy along the long axis to generally *decrease* with increasing distance. This should not be expected due to increased scatter for increasing distances that would tend to reduce the effects of anisotropy. Thus, the Monte Carlo results of Solberg *et al.*[36] are recommended as the ${}_{\mathrm{CON}}F(r,\theta)$ as in Table VII.

F. Mills Biopharmaceuticals Corporation model SL-125/SH-125 ^{125}I source

Mills Biopharmaceuticals originally introduced the model SL-125 (ProstaSeed®) ^{125}I source in 1999 and was acquired by Mentor Corporation in early 2003. The source is encapsulated in a 0.05-mm-thick Ti tube with a measured external length of 4.5 mm, an average measured outer diameter of 0.8 mm, and an end-weld thickness of 0.3 mm (Fig. 1). Internal source components include five 0.50-mm-diam silver spheres upon which a mixture containing radioactive iodine is adsorbed, similar to the process employed in production of the Amersham model 6711 seed. The deposition of radioactive iodine is nominally within several micrometers of the surface of the Ag sphere. Two published papers were reviewed to determine the full consensus dataset for the ProstaSeed®. Wallace presents comprehensive experimental measurements using lithium fluoride TLD 100 rods in PW2030 plastic water.[44] Li has published Monte Carlo calculations using version 7.3 of the PTRAN Monte Carlo code and the DLC-99 photon cross-section library for a $30\times30\times30$ cm^3 liquid water phantom.[45]

1. SL-125/SH-125 Λ

Wallace determined ${}_{\mathrm{EXP}}\Lambda$ using two calibration methods:[44] a ^{60}Co standard with corrections for photon energy response[46] and a cross calibration using NIST-traceable Amersham model 6711 and 6702 ^{125}I seeds. Due to the relative methodology employed, the cross-calibration results were not included in ${}_{\mathrm{EXP}}\Lambda$. In addition, TLD measurements of Λ utilized $S_{K,N99}$ and were subject to the 1999 WAFAC anomaly. Thus, a +3.1% correction was applied to give ${}_{\mathrm{EXP}}\Lambda=0.9805$ cGy h^{-1} U^{-1}. Phantom correction factors were taken from an unpublished manuscript by Wallace. However, Wallace specified that correction factors varied between 1.002 at 0.5 cm and 0.99 at 10 cm and were 0.995 at 1 cm. Li's calculation of ${}_{\mathrm{MC}}\Lambda$ employed the once more collided flux estimator for points adjacent to the seed (<5 mm) and the bounded next flight dose estimator for points beyond 5 mm.[45] In combination with the number of photon histories simulated, these estimators resulted in statistical uncertainties (1 σ) within 1.3% for all calculation points and distances. For ${}_{\mathrm{CON}}\Lambda$, Wallace's[44] measured value (multiplied by 1.031 to reflect the 1999 WAFAC measurement anomaly) was averaged with Li's[45] Monte Carlo estimate, yielding the 0.953 cGy h^{-1} U^{-1} value given in Table I. These two values agreed within 6%.

2. SL-125/SH-125 $g(r)$

Because Wallace[44] used a five-point geometry function and Li[45] employed the maximum extent of the radioactivity (0.29 cm) assuming 0.1 cm spacing between the pellets, $g_L(r)$ results for both studies were recalculated using $L_{\mathrm{eff}}=3.0$ mm according to Eq. (5) of the AAPM TG-43U1 report. Except for $r<0.5$ cm, good agreement with measured results by Wallace[44] is achieved between 0.5 and 7 cm, yielding maximum and minimum ratios of 1.13 and 0.90 at 4.0 and 7.0 cm, respectively. Due to the influence of volume-averaging effects at short distances, the $g(r)$ Monte Carlo data of Li[45] are recommended as consensus data (Table II).

3. SL-125/SH-125 $F(r,\theta)$

After conversion to a common L_{eff}, the Li $F(r,\theta)$ Monte Carlo data[45] were compared to the Wallace measured data.[44] Good agreement of $F(r,\theta)$ between Monte Carlo results and measured results for radial distances of 1, 2, 3, 4, and 5 cm is observed, often within 6%. The Li[45] data covered the distance range from 1 to 5.0 cm and were smooth and continuous in comparison to the measured result. Furthermore, the measured $F(r,\theta)$ data exhibited a different trend near the transverse plane in comparison to the calculated result, e.g., average differences of 6%, 8%, and 7% at 60°, 70°, and 80°, respectively. Thus, the Monte Carlo data of Li[45] are recommended as the consensus data set (Table VIII).

G. Source Tech Medical model STM1251 ^{125}I source

The Model STM1251 ^{125}I interstitial source was introduced to the market in 2002 by Source Tech Medical, who manufactured and marketed the source under the trade name

"^{125}Implant Seed." In 2003, C.R. Bard acquired the assets of Source Tech Medical and now markets the source. The model STM1251 source core (see Fig. 1) consists of a right circular cylinder of aluminum (0.51 mm diameter by 3.81 mm long) in which a 0.36-mm-diam gold radiographic marker is embedded. The aluminum cylinder is coated with 2-μm-thick inner and outer layers of nickel and copper, respectively, upon which a very thin (17 nm) layer of radioactive and cold iodine is deposited. The core is encapsulated in a titanium shell that is somewhat thicker than usual (0.08 mm radial thickness) but with very thin 0.13-mm-thick end caps. The external dimensions of the source are similar to those of other seeds.

The first published paper on model STM1251 dosimetry is a complete Monte Carlo study by Kirov and Williamson[47,48] in 2001 based upon the photon-transport code, PTRAN_CCG (version 7.44) using the DLC146 photon cross-section library and the corresponding mass-energy absorption coefficients.[17] The model was placed at the center of a 30-cm-diam liquid-water sphere and the radial dose function calculated over the 0.1–14 cm distance range. The 2D anisotropy functions were calculated over the 0.25–7 cm distance at 1°–5° angular intervals. The dose-rate constant was calculated using both extrapolation from transverse-plane point kerma-rate estimates (Λ_{extr}) and explicit simulation of the WAFAC standard (Λ_{WFC}) to estimate the air-kerma strength/contained activity ratio. Two experimental dosimetry studies, utilizing TLD-100 dosimeters in SolidWater™ phantom material, were subsequently published.[49,50] The Li and Williamson study[49] was based upon three seeds calibrated against the $S_{K,N99}$ standard (as revised in 2000) by an ADCL. The study was limited to the transverse plane, and the PTRAN calculational model used by Kirov and Williamson[47] was used to derive SolidWater™-to-liquid water corrections based upon the vendor's estimate of SolidWater™ composition. A standard distance-independent relative energy response correction of 1.41 was used. The TLD investigation of Chiu-Tsao *et al.*[50] included 2D anisotropy function measurements at 1, 2, 3, and 5 cm distances as well as partial measurements at 0.5 and 1.5 cm. Using the same Monte Carlo simulation approach as Kirov and Williamson,[47] the relative energy response function, $E(r)$, was calculated for the transverse axis measurement positions based upon the measured chemical composition of their SolidWater™ phantom (which had a calcium content about 10% lower than the vendor's specified concentration). The dependence of $E(r)$ on polar angle was not investigated. Eight seeds, calibrated against the $S_{K,N99}$ standard (as revised in 2000), were used to measure the dose-rate constant. For $r=1$ cm detector locations, 28 TLD readings from eight seeds were obtained while 18 readings from three seeds were obtained at other distances.

1. STM1251 Λ

Li and Williamson reported a measured Λ in water of 1.039 ± 0.075 cGy h^{-1} U^{-1} excluding uncertainties associated with SolidWater™ composition.[49] Chiu-Tsao *et al.* reported a somewhat higher value of 1.07 ± 0.06 cGy h^{-1} U^{-1} although their uncertainty analysis did not appear to include uncertainties associated with $E(r)$.[50] Based on the PTRAN calculations, described above, Kirov and Williamson reported Λ_{extr} and Λ_{WFC} values of 1.041 ± 0.026 and 0.982 ± 0.025 cGy h^{-1} U^{-1}, respectively.[47,48] The discrepancy between the point-detector extrapolation and WAFAC simulation methods was attributed to the fact that the right cylindrically shaped core is coated with a radio-opaque layer upon which the radioactive material is deposited. Similar to the model 200 ^{103}Pd and model 6711 ^{125}I seeds,[2,51] this induces polar anisotropy near the transverse axis at typical calibration distances due to self-absorption of radiation emitted by the radioactivity on the circular end surfaces of the core. Because the high atomic number Cu and Ni layers are so thin, they do not significantly attenuate ^{125}I x rays at short distances of 1–3 cm. In support of this explanation, the authors demonstrate that in-air profiles at 30 cm reveal "anisotropy overshoot" of 5% near the transverse axis. Polar dose profiles in medium also revealed subtle discontinuities that could be explained by screening of radioactivity on the core end surfaces. The error analysis by Kirov and Williamson included the influence of underlying cross-section uncertainties. To estimate a consensus dose-rate constant, ${}_{CON}\Lambda$, the two TLD measurements were averaged to yield ${}_{EXP}\Lambda=1.055$ cGy h^{-1} U^{-1}. This was averaged with the Monte Carlo estimate of Λ_{WFC}, yielding ${}_{CON}\Lambda=1.018$ cGy h^{-1} U^{-1}.

2. STM1251 $g(r)$

All three studies[47–50] used a simple line source model with $L=3.81$ mm to evaluate the geometry function, $G_L(r,\theta)$. Both Li and Williamson[49] and Chiu-Tsao *et al.*[50] corrected their TLD readings for the line-source geometry function and applied SolidWater™-to-liquid water corrections derived from PTRAN Monte Carlo calculations using the same geometric model of the seed. Li and Williamson[49] estimated $g_L(r)$ uncertainties to range from 3% to 10% while Chiu-Tsao *et al.*[50] claimed that $g(r)$ and $F(r,\theta)$ functions derived from TLD measurements had uncertainties of 2% at all distances. The Chiu-Tsao *et al.*[50] article also states that overall measurement uncertainty was 8% or less at all detector locations. Both reports[49,50] provided $g_L(r)$ at distances of 0.5–5 cm. A comparison of the three datasets reveals moderately good agreement between TLD measurements and the Monte Carlo calculations. At distances greater than 2 cm, Li and Williamson's[49] radial dose function is systematically more penetrating than that derived from the Monte Carlo calculations, by 5% at 2 cm to 13% at 5 cm. Li and Williamson[49] hypothesized that this discrepancy was due to errors in the solid-to-liquid correction function, which was based upon the vendor's specified composition which others have shown overestimates SolidWater™ calcium content.[52,53] Results by Chiu-Tsao *et al.*[50] for $g_L(r)$ are also larger than the Monte Carlo counterpart by 5%–6% in the 3–5 cm distance range. However, Kirov and Williamson's[47,48] $g_L(r)$ function agrees with the consensus radial dose function for the model 6702 seed,[2] also based

upon PTRAN Monte Carlo calculations, within 2%. This was an expected finding since there is no reason to believe that the STM1251 photon spectrum should significantly differ from that of the model 6702 seed. Thus Kirov and Williamson's Monte Carlo data are recommended for $_{CON}g(r)$.[47]

3. STM1251 $F(r,\theta)$

A comparison of $F(r,\theta)$ data from Chiu-Tsao *et al.*[50] with the corrected Monte Carlo data published by Kirov and Williamson[48] shows excellent agreement (2%–5%) at all angles and distances except the longitudinal axis ($\theta=0$). The agreement is especially good at 1 cm, which is Chiu-Tsao *et al.*'s highest precision dataset.[50] The poor agreement (19%–46% differences) on the longitudinal axis may be due to the very large dose gradients in this region (30%–40% dose reduction in a 1° interval, corresponding to a 0.2–1 mm spatial increment depending on distance), which are caused by self-absorption of the primary photons emitted from the cylindrical surface of the core. The Monte Carlo simulation used a point-kerma estimator to score dose and is able to accurately resolve rapidly changing dose distributions.[38] However, TLD measurements from Chiu-Tsao *et al.*[50] were corrected for volume averaging only on the transverse axis, where gradients are much smaller. The TLD and Monte Carlo 1D anisotropy functions agree within experimental uncertainties. Thus the Monte Carlo data of Kirov and Williamson,[48] were selected for $_{CON}F(r,\theta)$.

H. Best Medical model 2335 ^{103}Pd source

The model 2335 consists of 6 ^{103}Pd-coated spherical polymer (composition by weight percent: C: 89.73%, H: 7.85%, O: 1.68%, and N: 0.74%) beads 0.56 mm in diameter, three on each side of a 1.2-mm-long tungsten x-ray marker, all contained within a double-wall titanium capsule of total thickness 0.08 mm. As shown in Fig. 1, the outside dimensions of the cylindrical capsule are 5 mm in length and 0.8 mm in diameter, where the rim of the outer capsule is laser welded to the wall of the inner capsule.

In 2001, Meigooni *et al.* published the results of both TLD measurements and Monte Carlo simulations of the dosimetric characteristics of the model 2335 source.[54] For the measurements, a total of 12 seeds from three-different batches were used to irradiate TLD chips ($1.0\times1.0\times1.0$ mm^3 and $3.1\times3.1\times0.8$ mm^3) placed in holes machined in SolidWater™ blocks $25\times25\times20$ cm^3. An energy response correction factor between the 6 MV calibration energy and ^{103}Pd of 1.4 was used. Monte Carlo simulations utilized the PTRAN v.6.3 code in both SolidWater™ and water. The DLC-99 photon cross section library, Hubbell and Seltzer mass-energy absorption coefficients,[17] and NCRP Report 58 primary photon spectrum (1985) were employed. Simulation data from 3×10^6 histories (divided into 75 batches) were combined using a distance and attenuation-average bounded next flight point kerma estimator. The air-kerma rate, s_K, was calculated at a distance of 5 cm and subsequently corrected for inverse square law to 1 cm.

In 2002, Peterson and Thomadsen published the results of TLD measurements on the model 2335 source.[53] The ^{103}Pd source was mounted in the center of a Virtual Water™ (MED-CAL, Inc.) phantom on a rotating insert, allowing the source to be positioned at any angle with respect to the TLDs. Six phantoms were constructed from pairs of $15.2\times15.2\times5.0$ cm^3 blocks (28 TLD holes per block) which could accommodate 12 TLD cubes $1.0\times1.0\times1.0$ mm^3 ($r\leqslant1$ cm) and 16 TLD rods $1.0\times1.0\times3.0$ mm^3 ($r>1$ cm). Twenty three sources were used in 34 independent experiments, with a total of 28 TLDs for each run (two for each data point). Conversion factors from dose rate in SolidWater™-to-liquid water were obtained from Williamson.[55] One factor was used for each source-to-TLD distance, assumed to apply to Virtual Water due to the essentially identical chemical formulas of SolidWater™ and Virtual Water™. An energy response correction factor between the ^{60}Co (used for TLD calibration) and ^{103}Pd of 1.41 was used.

1. 2335 Λ

Meigooni *et al.*[54] reported a TLD-measured value of Λ in SolidWater™ of 0.67 ± 0.054 cGy h^{-1} U^{-1}, as well as an estimated TLD value of Λ in water of 0.69 ± 0.055 cGy h^{-1} U^{-1}. The latter was obtained by multiplying the measured value of Λ in SolidWater™ by 1.031, the ratio of the calculated value of Λ in water, 0.67 ± 0.02 cGy h^{-1} U^{-1}, to the calculated value of Λ in SolidWater™, 0.65 ± 0.02 cGy h^{-1} U^{-1}. Uncertainties in the TLD determination of Λ were quoted as having a Type A component of 4.0%, a Type B component of 5.5%, and a 2.5% uncertainty in S_K for a combined standard uncertainty of 7.2%. Uncertainty in the calculated values of Λ given above was estimated to be 1.5%, not including the component of uncertainty due to use of the DLC-99 cross section library.

Peterson and Thomadsen reported a TLD-measured value of 0.71 ± 0.07 cGy h^{-1} U^{-1} which was not impacted by the NIST WAFAC anomaly.[53] Uncertainties in Λ were quoted as having a Type A component of 10.0% ($n=10$) and a Type B component of 6.0% for a combined standard uncertainty of 11.7%. TLD measurements by Meigooni *et al.* were performed in SolidWater™, and produced in-phantom and in-water Λ values of 0.67 cGy h^{-1} U^{-1} and 0.69 cGy h^{-1} U^{-1}, respectively. As the calcium content (1.7% by mass) used for the in-phantom correction was only 0.6% less than the expected value, no significant change in the Meigooni *et al.* measured Λ values is expected beyond the experimental uncertainties (8%).[56] Therefore, $_{EXP}\Lambda=0.700$ cGy h^{-1} U^{-1} is based on the equally weighted average of Peterson and Thomadsen[53] and Meigooni *et al.*[56] measured values. Since the only calculated results (0.67 cGy h^{-1} U^{-1}) were from Meigooni *et al.* obtained at 5 cm by extrapolating to 1 cm on the transverse plane; these were used for $_{MC}\Lambda$. Consequently, $_{CON}\Lambda=0.685$ cGy h^{-1} U^{-1} (Table I).

2. 2335 $g(r)$

For calculating $G(r,\theta)$, Meigooni *et al.*[54] used the line source approximation with an effective length of $L_{\text{eff}}=4.25$ mm. To obtain $g(r)$, two sizes of TLDs were used at different distance ranges: 0.5–2 cm (small chips, 0.5 cm increments), 3–7 cm (large chips, 1 cm increments). The data reported for each distance was the average of that from at least eight TLD chips ($\sigma \cong 5\%$). Monte Carlo calculations were performed over a range of distances from 0.1 to 7 cm.

Peterson and Thomadsen determined $G(r,\theta)$ based on three different approximations of the radioactive material distribution within the source:[53]

1. Line source approximation, where the activity was assumed to be uniformly distributed over the length occupied by all active spheres ($L_{\text{eff}}=4.55$ mm),
2. Multi-point source approximation, where all active spheres were modeled as point sources, and
3. Point source approximation, where the source was modeled as a single point source. TLD measurements of $g(r)$ were made over a range of distances from 0.5 to 5 cm.

It was noted that the data appeared to be shifted from that of Meigooni *et al.*,[54] which lead Peterson and Thomadsen[53] to investigate the cause of the disagreement. The results of phantom material chemical analysis performed by Peterson and Thomadsen indicated a difference in calcium content (Virtual Water=2.4% vs. Solid Water™=1.7%, compared to the expected value of 2.3%) between the two phantom materials. Phantom construction and $G(r,\theta)$ were also noted as additional factors which possibly contributed to disagreement between the datasets.

To determine ${}_{\text{CON}}g(r)$, the data measured using TLDs from Meigooni *et al.*[54] were first corrected from SolidWater™-to-liquid water using factors provided by Williamson.[55] There were no details given by Meigooni *et al.*[54] as to how their value of L_{eff} was determined (which differed from that of Peterson and Thomadsen), whereas the value given by Peterson and Thomadsen[53] agreed with that obtained using the calculation method published in TG-43U1. Therefore, measured and calculated datasets from Meigooni *et al.* were then reprocessed using $L_{\text{eff}}=4.55$ mm. Ratios of $g_L(r)$ values from TLD measurements by Peterson and Thomadsen[53] and Monte Carlo calculations by Meigooni *et al.*[54] were within ±9% for all values of r. ${}_{\text{CON}}g(r)$ was formed by combining Monte Carlo-calculated values from Meigooni *et al.* from $r=0.1$ to 0.4 cm and $r=5.5$–7 cm with the Peterson and Thomadsen line source approximation dataset from $r=0.5$ to 5 cm.[53,57]

3. 2335 $F(r,\theta)$

The anisotropy function was measured by Meigooni *et al.*[54] using TLDs placed at distances of $r=2$, 3, and 5 cm from the source, with θ in 10° intervals relative to the source axis. Each point of $F(r,\theta)$ was based on the average of data from at least eight TLD chips. Their Monte Carlo calculations were conducted over a range of distances from $r=1$ to 7 cm from the source, with θ in 5° increments relative to the source axis. The uncertainty in the calculations (component due to use of the DLC-99 cross section library not included) was estimated to be 1.5% for $r<3$ cm, and 5%–6% for $r>5$ cm.

TLD measurements of $F(r,\theta)$ by Peterson and Thomadsen used a range of angles from 0° to 165°.[53] The line source approximation for $G(r,\theta)$ was used. The ratios of $F(r,\theta)$ values from the TLD measurements of Peterson and Thomadsen and the Monte Carlo calculations of Meigooni *et al.*[54] were within ±13% for all values of r and θ. Due to the finer angular resolution of the Monte Carlo calculated values of $F(r,\theta)$ by Meigooni *et al.* compared to both sets of TLD measurements, ${}_{\text{CON}}F(r,\theta)$ was taken from Meigooni *et al.* and reprocessed using $L_{\text{eff}}=4.55$ mm.

[a]Electronic mail: mrivard@tufts-nemc.org

[1]R. Nath, L. L. Anderson, G. Luxton, K. A. Weaver, J. F. Williamson, and A. S. Meigooni, "Dosimetry of interstitial brachytherapy sources: Recommendations of the AAPM Radiation Therapy Committee Task Group No. 43," Med. Phys. **22**, 209–234 (1995).
[2]M. J. Rivard, B. M. Coursey, L. A. DeWerd, W. F. Hanson, M. S. Huq, G. S. Ibbott, M. G. Mitch, R. Nath, and J. F. Williamson, "Update of AAPM Task Group No. 43 Report: A revised AAPM protocol for brachytherapy dose calculations," Med. Phys. **31**, 633–674 (2004).
[3]M. J. Rivard, W. M. Butler, L. A. DeWerd, M. S. Huq, G. S. Ibbott, Z. Li, M. G. Mitch, R. Nath, and J. F. Williamson, "Erratum: Update of AAPM Task Group No. 43 Report: A revised AAPM protocol for brachytherapy dose calculations [Med. Phys. 31, 633–674 (2004)]," Med. Phys. **31**, 3532–3533 (2004).
[4]J. F. Williamson, W. Butler, L. A. DeWerd, M. S. Huq, G. S. Ibbott, Z. Li, M. G. Mitch, R. Nath, M. J. Rivard, and D. Todor, "Recommendations of the American Association of Physicists in Medicine regarding the impact of implementing the 2004 Task Group 43 report on dose specification for ^{103}Pd and ^{125}I interstitial brachytherapy," Med. Phys. **32**, 1424–1439 (2005).
[5]A. S. Meigooni, V. Rachabatthula, S. B. Awan, and R. A. Koona, "Comments on: Update of AAPM Task Group No. 43 Report: A revised AAPM protocol for brachytherapy dose calculations [Med. Phys. **31**, 633–674 (2004)]," Med. Phys. **32**, 1820–1821 (2005).
[6]M. J. Rivard, W. Butler, L. A. DeWerd, M. S. Huq, G. S. Ibbott, C. S. Melhus, M. G. Mitch, R. Nath, and J. F. Williamson, "Response to 'Comment on Update of AAPM Task Group No. 43 Report: A revised AAPM protocol for brachytherapy dose calculations,"' Med. Phys. **32**, 1822–1824 (2005).
[7]J. F. Williamson, B. M. Coursey, L. A. DeWerd, W. F. Hanson, and R. Nath, "Dosimetric prerequisites for routine clinical use of new low energy photon interstitial brachytherapy sources," Med. Phys. **25**, 2269–2270 (1998).
[8]L. A. DeWerd, M. S. Huq, I. J. Das, G. S. Ibbott, W. F. Hanson, T. W. Slowey, J. F. Williamson, and B. M. Coursey, "Procedures for establishing and maintaining consistent air-kerma strength standards for low-energy, photon-emitting brachytherapy sources: Recommendations of the Calibration Laboratory Accreditation Subcommittee of the American Association of Physicists in Medicine," Med. Phys. **31**, 675–681 (2004).
[9]Radiological Physics Center, The M.D. Anderson Cancer Center, Houston, Texas http://rpc.mdanderson.org/rpc/ last accessed May 11, 2007.
[10]M. J. Rivard, "Refinements to the geometry factor used in the AAPM Task Group Report No. 43 necessary for brachytherapy dosimetry calculations," Med. Phys. **26**, 2445–2450 (1999).
[11]M. J. Rivard, C. S. Melhus, and B. L. Kirk, "Brachytherapy dosimetry parameters calculated for a new ^{103}Pd source," Med. Phys. **31**, 2466–2470 (2004).
[12]J. Pérez-Calatayud, D. Granero, and F. Ballester, "Phantom size in brachytherapy source dosimetric studies," Med. Phys. **31**, 2075–2081 (2004).
[13]C. S. Melhus and M. J. Rivard, "Approaches to calculating AAPM TG-43 brachytherapy dosimetry parameters for ^{137}Cs, ^{125}I, ^{192}Ir, ^{103}Pd, and ^{169}Yb

sources," Med. Phys. **33**, 1729–1737 (2006).
[14]E. E. Furhang and L. L. Anderson, "Functional fitting of interstitial brachytherapy dosimetry data recommended by the AAPM Radiation Therapy Committee Task Group 43. American Association of Physicists in Medicine," Med. Phys. **26**, 153–160 (1999).
[15]K. T. Sowards and A. S. Meigooni, "A Monte Carlo evaluation of the dosimetric characteristics of the EchoSeed™ model 6733 ^{125}I brachytherapy source," Brachytherapy **1**, 227–232 (2002).
[16]A. S. Meigooni, S. A. Dini, K. Sowards, J. L. Hayes, and A. Al-Otoom, "Experimental determination of the TG-43 dosimetric characteristics of EchoSeed™ model 6733 ^{125}I brachytherapy source," Med. Phys. **29**, 939–942 (2002).
[17]J. H. Hubbell and S. M. Seltzer, "Tables of x-ray mass attenuation coefficients and mass energy-absorption coefficients 1 keV to 20 MeV for elements Z=1 to 92 and 48 additional substances of dosimetric interest," NISTIR 5632 (1995).
[18]J. F. Williamson, "Comparison of measured and calculated dose rates in water near ^{125}I and ^{192}Ir seeds," Med. Phys. **18**, 776–785 (1991).
[19]R. Nath and N. Yue, "Dosimetric characterization of a newly designed encapsulated interstitial brachytherapy source of iodine-125-model LS-1 Brachyseed™," Appl. Radiat. Isot. **55**, 813–821 (2001).
[20]A. S. Meigooni, J. A. Meli, and R. Nath, "A comparison of solid phantoms with water for dosimetry of ^{125}I model 6702 brachytherapy sources," Med. Phys. **15**, 695–701 (1998).
[21]G. H. Chan and W. V. Prestwich, "Dosimetric properties of the new ^{125}I BrachySeed™ model LS-1 source," Med. Phys. **29**, 190–200 (2002).
[22]J. F. Williamson, "Dosimetric characteristics of the DRAXIMAGE model LS-1 interstitial brachytherapy source design: A Monte Carlo investigation," Med. Phys. **29**, 509–521 (2002).
[23]R. Wang and R. S. Sloboda, "Monte Carlo dose parameters of the BrachySeed model LS-1 ^{125}I brachytherapy source," Appl. Radiat. Isot. **56**, 805–813 (2002).
[24]G. H. Chan, R. Nath, and J. F. Williamson, "On the development of consensus values of reference dosimetry parameters for interstitial brachytherapy sources," Med. Phys. **31**, 1040–1045 (2004).
[25]J. F. Williamson, personal communication, December 2004.
[26]D. M. Duggan and B. L. Johnson, "Dosimetry of the I-Plant Model 3500 iodine-125 brachytherapy source," Med. Phys. **28**, 661–670 (2001).
[27]R. E. Wallace, "Model 3500 ^{125}I brachytherapy source dosimetric characterization," Appl. Radiat. Isot. **56**, 581–587 (2002).
[28]M. J. Rivard, "Comprehensive Monte Carlo calculations of AAPM Task Group Report No. 43 dosimetry parameters for the Model 3500 I-Plant ^{125}I brachytherapy source," Appl. Radiat. Isot. **57**, 381–389 (2002).
[29]D. M. Duggan, "Improved radial dose function estimation using current version MCNP Monte-Carlo simulation: Model 6711 and ISC3500 ^{125}I brachytherapy source," Appl. Radiat. Isot. **61**, 1443–1450 (2004).
[30]B. Reniers, S. Vynckier, and P. Scalliet, "Dosimetric study of the new InterSource^{125} iodine seed," Med. Phys. **28**, 2285–2288 (2001).
[31]B. Reniers, F. Verhaegen, and S. Vynckier, "The radial dose function of low-energy brachytherapy seeds in different solid phantoms: comparison between calculations with the EGSnrc and MCNP4C Monte Carlo codes and measurements," Phys. Med. Biol. **49**, 1569–1582 (2004).
[32]A. S. Meigooni, M. M. Yoe-Sein, A. Y. Al-Otoom, and K. T. Sowards, "Determination of the dosimetric characteristics of InterSource^{125} iodine brachytherapy source," Appl. Radiat. Isot. **56**, 589–599 (2002).
[33]B. Reniers, private communication, May 26, 2006.
[34]A. S. Meigooni, J. L. Hayes, H. Zhang, and K. Sowards, "Experimental and theoretical determination of dosimetric characteristics of IsoAid ADVANTAGE™ ^{125}I brachytherapy source," Med. Phys. **29**, 2152–2158 (2002).
[35]A. S. Meigooni, J. L. Hayes, H. Zhang, and K. Sowards, "Erratum: Experimental and theoretical determination of dosimetric characteristics of IsoAid ADVANTAGE™ ^{125}I brachytherapy source [Med. Phys. **29**, 2152–2158 (2002)]," Med. Phys. **30**, 279 (2003).
[36]T. D. Solberg, J. J. DeMarco, G. Hugo, and R. E. Wallace, "Dosimetric parameters of three new solid core I-125 brachytherapy sources," J. Appl. Clin. Med. Phys. **3**, 119–134 (2002).
[37]P. J. Muench, A. S. Meigooni, R. Nath, and W. L. McLaughlin, "Photon energy dependence of the sensitivity of radiochromic film and comparison with silver halide film and LiF TLDs used for brachytherapy dosimetry," Med. Phys. **18**, 769–775 (1991).
[38]J. F. Williamson, "Monte Carlo evaluation of kerma at a point for photon transport problems," Med. Phys. **14**, 567–576 (1987).
[39]M. J. Berger and J. J. Hubbell, "XCOM: Photon cross sections on a personal computer," National Bureau of Standards Internal Report No. 87, 3597 (1987).
[40]S. M. Seltzer, "Calculation of photon mass-energy transfer and mass-energy absorption coefficients," Radiat. Res. **136**, 147–170 (1993).
[41]E. Kouwenhoven, R. van der Laars, and D. R. Schaart, "Variation in interpretation of the AAPM TG-43 geometry factor leads to unclearness in brachytherapy dosimetry," Med. Phys. **28**, 1965–1966 (2001).
[42]J. A. Meli, "Let's abandon geometry factors other than that of a point source in brachytherapy dosimetry," Med. Phys. **29**, 1917–1918 (2002).
[43]M. J. Rivard, B. M. Coursey, L. A. DeWerd, W. F. Hanson, M. S. Huq, G. Ibbott, R. Nath, and J. F. Williamson, "Comment on: Let's abandon geometry factors other than that of a point source in brachytherapy dosimetry," Med. Phys. **29**, 1919–1920 (2002).
[44]R. E. Wallace, "Empirical dose characterization of model I125-SL ^{125}Iodine brachytherapy source in phantom," Med. Phys. **27**, 2796–2802 (2000).
[45]Z. Li, "Monte Carlo calculations of dosimetry parameters of the Urocor ProstaSeed ^{125}I source," Med. Phys. **29**, 1029–1034 (2002).
[46]K. A. Weaver, V. Smith, D. Huang, C. Barnett, M. C. Schell, and C. C. Ling, "Dose parameters of ^{125}I and ^{192}Ir seed sources," Med. Phys. **16**, 636–643 (1989).
[47]A. S. Kirov and J. F. Williamson, "Monte Carlo-aided dosimetry of the Source Tech Medical Model STM1251 I-125 interstitial brachytherapy source," Med. Phys. **28**, 764–772 (2001).
[48]A. S. Kirov and J. F. Williamson, "Erratum: Monte Carlo-aided dosimetry of the Source Tech Medical Model STM1251 I-125 interstitial brachytherapy source [Med. Phys. **28**, 764–772 (2001)]," Med. Phys. **29**, 262–263 (2002).
[49]Z. Li and J. F. Williamson, "Measured transverse-axis dosimetric parameters of the model STM1251 ^{125}I interstitial source," J. Appl. Clin. Med. Phys. **3**, 212–217 (2002).
[50]S-T. Chiu-Tsao, T. L. Duckworth, C-Y. Hsiung, Z. Li, J. F. Williamson, N. S. Patel, and L. B. Harrison, "Thermoluminescent dosimetry of the SourceTech Medical model STM1251 ^{125}I seed," Med. Phys. **30**, 1732–1735 (2003).
[51]J. I. Monroe and J. F. Williamson, "Monte Carlo-aided dosimetry of the Theragenics TheraSeed model 200 ^{103}Pd interstitial brachytherapy seed," Med. Phys. **29**(4), 609–21 (2002).
[52]N. S. Patel *et al.*, "Thermoluminescent dosimetry of the Symmetra ^{125}I model I25. S06 interstitial brachytherapy seed," Med. Phys. **28**, 1761–1769 (2001).
[53]S. W. Peterson and B. Thomadsen, "Measurements of the dosimetric constants for a new ^{103}Pd brachytherapy source," Brachytherapy **1**, 110–119 (2002).
[54]A. S. Meigooni, Z. Bharucha, M. Yoe-Sein, and K. Sowards, "Dosimetric characteristics of the Best® double-wall ^{103}Pd brachytherapy source," Med. Phys. **28**, 2568–2575 (2001).
[55]J. F. Williamson, personal communication, December 2001.
[56]A. S. Meigooni, S. B. Awan, N. S. Thompson, and S. A. Dini, "Updated Solid Water™ to water conversion factors for ^{125}I and ^{103}Pd brachytherapy sources," Med. Phys. **33**, 3988–3992 (2006).
[57]S. W. Peterson and B. Thomadsen, "Erratum: Measurements of the dosimetric constants for a new ^{103}Pd brachytherapy source," Brachytherapy **1**, 233 (2002).